INSTITUTE OF PHYSICS PUBLISHING JOURNAL OF PHYSICS: CONDENSED MATTER

J. Phys.: Condens. Matter **17** (2005) R217–R252 doi:10.1088/0953-8984/17/4/R03

TOPICAL REVIEW

Negative thermal expansion

G D Barrera[1], J A O Bruno[2], T H K Barron[3] and N L Allan[3]

[1] Departamento de Química, Universidad Nacional de la Patagonia SJB, Ciudad Universitaria, 9000 Comodoro Rivadavia, Argentina
[2] Universidad de Buenos Aires, Facultad de Ciencias Exactas y Naturales, Departamento de Química Inorgánica, Analítica y Química Física, Pabellón 2, Ciudad Universitaria, 1428 Buenos Aires, Argentina
[3] School of Chemistry, University of Bristol, Cantock's Close, Bristol BS8 1TS, UK

Received 30 October 2004
Published 14 January 2005
Online at stacks.iop.org/JPhysCM/17/R217

Abstract

There has been substantial renewed interest in negative thermal expansion following the discovery that cubic ZrW_2O_8 contracts over a temperature range in excess of 1000 K. Substances of many different kinds show negative thermal expansion, especially at low temperatures. In this article we review the underlying thermodynamics, emphasizing the roles of thermal stress and elasticity. We also discuss vibrational and non-vibrational mechanisms operating on the atomic scale that are responsible for negative expansion, both isotropic and anisotropic, in a wide range of materials.

Contents

1. Introduction

Not all substances expand on heating. Probably the most familiar example of negative thermal expansion from everyday life is the increase in density of liquid water between 0 and 4 °C, which is crucial for the preservation of aquatic life during very cold weather. The phenomenon is however found more often in solids, and interest in the underlying reasons for this apparently anomalous behaviour has been renewed by the work of Sleight and colleagues [1, 2] on cubic zirconium tungstate, which is found to contract on heating from below 15 K up to its decomposition temperature of ≈1500 K. Two excellent reviews by Sleight [3] and Evans [4] have concentrated mainly on this and related 'framework' materials. The purpose of this article is to present a more general (though still necessarily incomplete) survey of negative thermal expansion over a *wide* range of solid materials, highlighting thermodynamics and diverse mechanisms operating at the atomic level.

Negative thermal expansion has been studied experimentally and theoretically for decades (e.g. [5–14]). Among materials with this property are Si and Ge and other tetrahedrally bonded crystals at low temperature, β-quartz at high temperature, some ceramics and zeolites with framework structures (the latter predicted prior to experiment!) and related glasses, and C_{60} [15]. Many other solids on heating expand in some directions and contract in others, such as some metals and alloys, calcite [16], α-quartz at very low temperatures, some ferroelectric resistors which are perovskite solid solutions $A(M'M'')O_3$ [17], some high-T_c superconductors such as $YBa_2Cu_3O_{7-\delta}$, crystalline polyethylene and other crystalline polymers, and graphite fibre-reinforced polymers. Systems with practical applications [12] include Invar, β-eucryptite, cordierite ($Mg_2Al_2Si_5O_{18}$), β-spodumene and the NZP family. Uses range from precision instruments and astronomical telescope mirrors to casserole dishes and stove-tops. One useful procedure is to mix materials having negative expansion with others having positive expansion so as to obtain a net expansion of approximately zero.

The contraction of solids on heating seems anomalous because it offends the intuitive concept that atoms need more room as vibrational amplitudes increase. A popular textbook explanation (e.g. [18]) for thermal expansion is based on a model of anharmonic pair potentials between atoms in the solid (figure 1). When the atoms vibrate along a line connecting the pair, the asymmetry in the potential causes an increase in the mean distance between the atoms as the temperature increases. This crude picture does indeed reveal the most important mechanism for positive thermal expansion, and indicates correctly that atomic vibrations give rise to thermal expansion only because of anharmonicity. But it cannot account for negative thermal expansion, because it considers only the component of relative vibrational motion directed along the line joining the atoms. We shall see in section 2.2.2(b) that relative motion perpendicular to this line tends to decrease the distance between the mean positions of the two atoms, and so to contract the solid. In addition, non-vibrational contributions (electronic, nuclear etc) to the thermodynamic properties can also cause spectacular effects, particularly at low temperatures where vibrational contributions are small.

We first consider cubic and isotropic materials, where the expansion is isotropic. A summary of the relevant thermodynamics is followed by a discussion of vibrational mechanisms, illustrated by examples. In non-cubic materials thermal stresses and elasticity are both anisotropic; thermal expansion results from the interplay between them, leading to a rich variety of behaviour. The underlying vibrational mechanisms can sometimes be elucidated by computer simulation techniques, notably quasi-harmonic lattice dynamics. We consider more briefly electronic and other non-vibrational effects, and finally interfaces and nanoparticles.

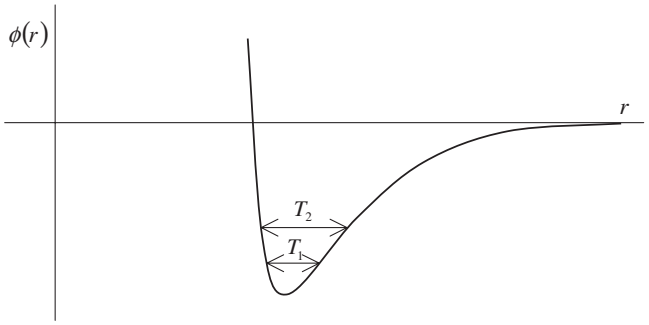

Figure 1. A typical anharmonic pair potential ϕ, as a function of interatomic distance r, showing mean amplitudes of vibration at two different temperatures ($T_2 > T_1$), indicating positive thermal expansion.

2. Cubic and isotropic materials

2.1. Thermodynamics

The volume V of any substance under external pressure P_0 at any temperature is that which minimizes the 'availability' [19] $F(V, T) + P_0V$, where F is the Helmholtz energy. Figure 2 plots schematically the variation of $F + P_0V$ with V at two temperatures, for (a) positive and (b) negative thermal expansion. The volumes marked explicitly on the V-axis give the minima of each $F + P_0V$ versus V isotherm, and thus are the equilibrium volumes at temperatures T and $T + \delta T$ respectively. We see that the position of a minimum will change with temperature only if the entropy depends on the volume.

The relation to the volume dependence of the entropy can also be seen by applying standard thermodynamic transformations to the *volumetric thermal expansion coefficient* β, defined by

$$\beta = \frac{1}{V}\left(\frac{\partial V}{\partial T}\right)_P. \tag{1}$$

By a Maxwell relation,

$$\beta = \frac{1}{V}\left(\frac{\partial V}{\partial T}\right)_P = -\frac{1}{V}\left(\frac{\partial S}{\partial P}\right)_T = \chi_T\left(\frac{\partial S}{\partial V}\right)_T \tag{2}$$

where χ_T is the isothermal compressibility $-(\partial V/\partial P)_T/V$. The compressibility is always positive, and so the change in volume on heating will always be in the direction of increasing entropy; a negative β thus indicates that the entropy increases when the substance is compressed isothermally. Entropy (disorder) would *normally* be expected to increase with volume, and usually β is indeed positive. It is only in this limited sense that negative thermal expansion is 'anomalous'. For an ideal classical or quantum gas, β is always positive; the origin of negative thermal expansion must therefore lie in the interactions between the particles. For example, the negative expansion of liquid water below 4 °C is associated with an increase of entropy on compression due to break-up of tetrahedral H bonding, which over this temperature range more than compensates for effects tending to decrease the entropy.

Further insight is obtained by transforming equation (2) to

$$\beta = \chi_T\left(\frac{\partial P}{\partial T}\right)_V = \left(\frac{\partial P}{\partial T}\right)_V\left(\frac{-\partial \ln V}{\partial P}\right)_T \tag{3}$$

which expresses thermal expansion as the elastic response to thermally induced stress. Equation (3) shows that if we wish we can imagine thermal expansion as occurring in two

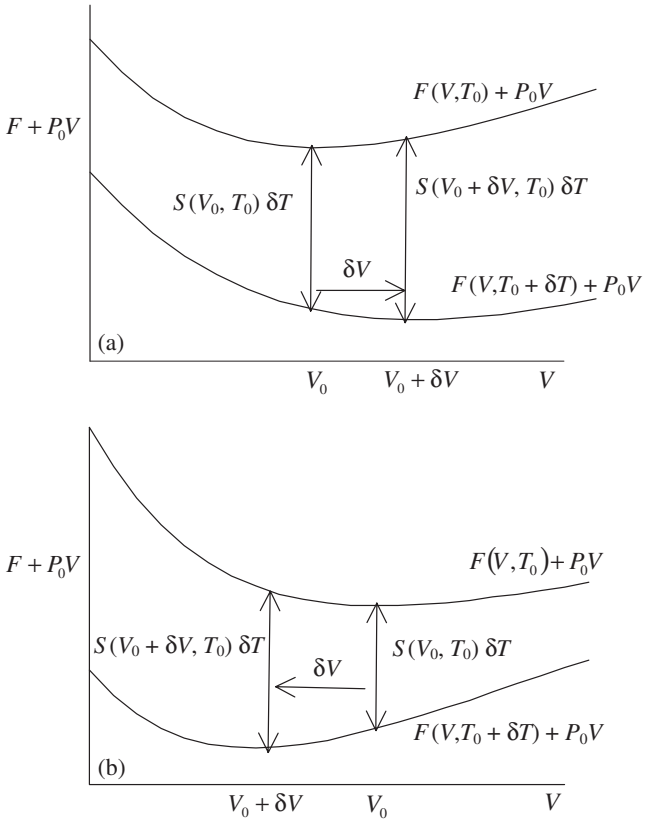

Figure 2. Thermodynamics of thermal expansion: (a) positive, (b) negative expansion. At constant pressure P_0, the volume at each temperature T is that which minimizes $F(V, T) + P_0 V$. Expansion is always in the direction of increasing entropy. Note also that $\left(\partial^2 F/\partial V^2\right)_T = 1/(V\chi_T)$, where χ_T is the isothermal compressibility.

stages: first, a change in pressure, as the temperature is increased at constant volume; after that, a change in volume, as the material is allowed to relax to the original pressure at the higher temperature. As $T \to 0$ the compressibility approaches a finite limit, and so at low temperatures the temperature dependence of β is like that of the *thermal pressure coefficient* $(\partial P/\partial T)_V$.

2.1.1. Grüneisen functions. $(\partial P/\partial T)_V$ in equation (3) may in turn be expressed as the product of two factors: the heat capacity per unit volume, C_V/V, which determines how much energy the material gains during a given temperature increase, and the thermodynamic Grüneisen function, γ, which determines the effectiveness of that energy in changing the pressure:

$$\left(\frac{\partial P}{\partial T}\right)_V = \left(\frac{C_V}{V}\right)\gamma \tag{4}$$

where

$$\gamma = \left(\frac{\partial P}{\partial (U/V)}\right)_V = -\left(\frac{\partial \ln T}{\partial \ln V}\right)_S \tag{5}$$

and U is the internal energy. Combining equations (3) and (4) with the identity $\chi_T C_V = \chi_S C_P$ gives

$$\beta = (\chi_T C_V / V)\,\gamma = (\chi_S C_P / V)\,\gamma \tag{6}$$

where χ_S is the adiabatic compressibility and C_P is the heat capacity at constant pressure.

The Grüneisen function thus encapsulates the information given by measurements of thermal expansion not already given by the heat capacity and compressibility. In particular, its sign determines whether the expansion is positive or negative. γ is dimensionless, and for many simple materials varies little over a wide range about room temperature. Thanks to this, and partly too for historical reasons [20], γ is often referred to as the Grüneisen *constant*. But for many other solids γ varies greatly with temperature, and indeed plots of γ versus T are widely used in presenting both experimental and theoretical results. Such plots are particularly useful at low temperatures, where both β and C_V can change by many orders of magnitude, while γ usually remains of order unity. Experimental values of γ are usually obtained from measurements of β, C_P and χ_S:

$$\gamma = \beta V / \chi_S C_P. \tag{7}$$

2.1.2. Linear expansion coefficients. Most thermal expansion measurements on solids are of linear expansion coefficients α. These are defined in the same way[4] [21] as β, except that length l takes the place of volume V:

$$\alpha = (1/l)(\partial l / \partial T)_P. \tag{8}$$

For isotropic or cubic symmetry the linear expansion is independent of direction, and the coefficients of volumetric and linear expansion are simply related by $\beta = 3\alpha$. For lower symmetry the linear expansion varies with direction, requiring a more general treatment (section 3.2).

2.2. Vibrational mechanisms

Lattice vibrations (phonons) play a major part in thermal expansion, except for some materials at very low temperatures. It is usually a good approximation to regard the vibrations of a solid of N atoms as governed by a potential energy which is a $3N$-dimensional function of the atomic displacements; for insulators, this is given by the Born–Oppenheimer approximation [22]. It is a many-body potential, although effective pair potentials between neighbouring atoms are often dominant and have formed the basis for much theoretical work.

Thermal expansion of solids occurs because the $3N$-dimensional potential is anharmonic (see [21, section 1.7.8.1] and [23]). Each atom i vibrates about its mean position $\langle \mathbf{r}_i \rangle$, but distances between these mean positions change with temperature. We must here distinguish between 'apparent' and 'true' bond lengths[5]. The apparent bond length, as obtained from x-ray or neutron diffraction measurements, is the distance between the mean positions of two atoms, $|\langle \mathbf{r}_2 \rangle - \langle \mathbf{r}_1 \rangle| = |\langle \mathbf{r}_2 - \mathbf{r}_1 \rangle|$, and hence is directly related to bulk thermal expansion. The true bond length, as given for example by radial distribution functions obtained from extended x-ray absorption fine structure [24], is the mean distance between the atoms, $\langle |\mathbf{r}_2 - \mathbf{r}_1| \rangle$. The apparent bond length is always shorter than the true bond length, because components of relative motion of the two atoms perpendicular to $\langle \mathbf{r}_2 - \mathbf{r}_1 \rangle$ contribute only to the latter. Negative expansion

[4] Slightly different definitions of expansion coefficients are sometimes used (see, e.g., [21]).

[5] In this context, 'bond' is used not only for intramolecular chemical bonds but also for weak physical interactions such as those involved in intermolecular interactions.

can therefore occur even when true bond lengths are increasing with temperature. We can also distinguish between apparent and true bond angles, but there is no general rule for which of these is the greater.

2.2.1. The quasi-harmonic approximation. To discuss vibrational effects in detail we use the quasi-harmonic approximation. To a first approximation the anharmonicity responsible for thermal expansion is adequately described by the volume dependence of frequencies of the lattice vibrations, which otherwise are treated as harmonic (e.g. [23]). The vibrational free energy, entropy and heat capacity are then sums of contributions f_j, s_j and c_j from independent vibrational modes of frequency $\omega_j(V)$; in particular, s_j and c_j depend only on $\hbar\omega_j/kT$. The volume derivatives of the ω_j are conveniently described by dimensionless 'mode Grüneisen parameters' γ_j defined by

$$\gamma_j = -\mathrm{d}\ln\omega_j/\mathrm{d}\ln V. \tag{9}$$

It can be shown that the thermal pressure coefficient is given by

$$\left(\frac{\partial P}{\partial T}\right)_V = \left(\frac{\partial S}{\partial V}\right)_T = \frac{1}{V}\sum_j c_j\gamma_j \tag{10}$$

where c_j is given by the well known Einstein specific heat function

$$c_j = k\left(\frac{\hbar\omega_j}{2kT}\right)^2 \mathrm{cosech}^2\left(\frac{\hbar\omega_j}{2kT}\right) = k\left(\frac{\hbar\omega_j}{kT}\right)^2 \Big/ [\{\exp(\hbar\omega_j/kT) - 1\} \times \{1 - \exp(-\hbar\omega_j/kT)\}]. \tag{11}$$

By equations (4) and (10), the thermodynamic Grüneisen function of equation (5) becomes an average of the γ_j weighted by the c_j:

$$\gamma = \sum_j c_j\gamma_j \Big/ \sum_j c_j. \tag{12}$$

If γ_j is negative, the frequency ω_j *increases* with volume and the contribution s_j to the entropy *decreases*. Thermal expansion is negative at a given temperature if there are enough such modes excited to outweigh those with positive γ_j.

The classical value of c_j is k for all modes, giving a high temperature limit γ_∞ for γ, equal to the arithmetic mean of all the γ_j. Typical experimental data show γ flattening off at about room temperature (e.g. figure 7). Much additional information is obtained from measurements at lower temperatures, which sample progressively the γ_j of only low frequency modes; this provides a stringent test of theoretical models. At very low temperatures the vibrational contributions to C_V and β fall off as T^3, and other contributions may become dominant (e.g. figures 12 and 15(b)).

2.2.2. Pair potential mechanisms. At the atomic level, what determines whether β is positive or negative? For pairwise interatomic potentials, three mechanisms [21, 25 (I: section 3.2)] have been distinguished:

(a) *The 'bond-stretching effect'*. This mechanism is due to the asymmetry of the pair potential; it has already been illustrated in figure 1, but we can now relate it to the Grüneisen parameters $\gamma_j = -\mathrm{d}\ln\omega_j/\mathrm{d}\ln V$. A mode j with a component of relative motion along a bond direction brings into play the stretching force constant $\phi''(r)$. Increasing the volume causes the bond to lengthen, thus weakening the force constant and tending to lower the frequency ω_j, so contributing *positively* to γ_j and the thermal expansion.

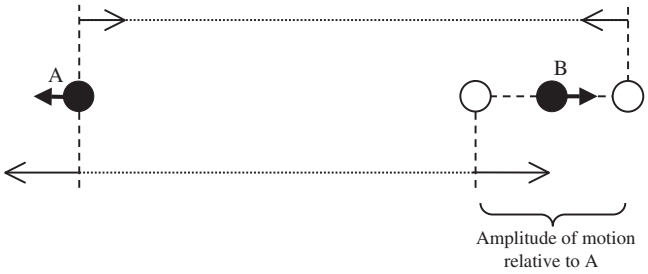

Figure 3. The bond-stretching effect. When the *mean* distance between atoms A and B is held constant, vibrations along the bond direction produce a net repulsive force: the pair potential is asymmetric (figure 1), and so the attraction when the atoms are further apart is smaller than the corresponding repulsion when they are closer together. →, instantaneous force; ⟶, time-averaged force.

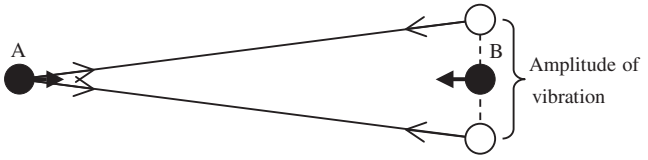

Figure 4. The tension effect. When the distance between the mean position of the atoms is held constant, a net attractive force is produced by relative thermal displacement with components normal to a pair potential based bond (see the text). →, instantaneous force; ⟶, time-averaged force.

Equivalently, we can consider $(\partial P/\partial T)_V$ directly. At constant volume, the distance r_0 between the atomic mean positions remains fixed. With increasing temperature the amplitude of vibration increases, but since r_0 is fixed r continues to sample values both less than and greater than r_0. Since the magnitude of the repulsion between the atoms when $r < r_0$ is greater than that of the attraction when $r > r_0$ (figure 3), there is a net repulsive force; this increases with temperature, contributing positively to $(\partial P/\partial T)_V$.

(b) *The 'tension effect'*. In possibly the earliest vibrational model giving negative thermal expansion [26, 27], Barron replaced the asymmetric pair potential of figure 1 by a symmetric Hooke's law potential, thus eliminating the bond-stretching mechanism. The thermal expansion of a cubic close-packed lattice then became not zero[6] but negative at all temperatures. This was due to an effect that occurs when there is a component of relative motion transverse to the direction of the bond (cf the second paragraph of section 2.2). It can be explained simply in terms of the Grüneisen parameters γ_j. An increase in volume increases tension in the bonds; the restoring force for transverse motion is thus enhanced, raising the frequency (as in a violin string) and so contributing *negatively* to γ_j and the thermal expansion.

Equivalently we can again consider $(\partial P/\partial T)_V$ directly. When the distance between the mean atomic positions remains fixed, relative motion transverse to the bond increases the time-averaged distance between the atoms, producing a mean attractive force (figure 4) and hence a negative contribution to $(\partial P/\partial T)_V$. At constant pressure, the elastic response is to reduce the crystal volume, thus decreasing the distance between the *mean positions*

[6] Like all vibrational mechanisms for thermal expansion, this is an anharmonic effect. Even when the *pair* potential is a harmonic function of the interatomic distance, it gives rise to an expression for the energy of the *crystal* that is an anharmonic function of the three-dimensional atomic displacements (see [21, p 68]).

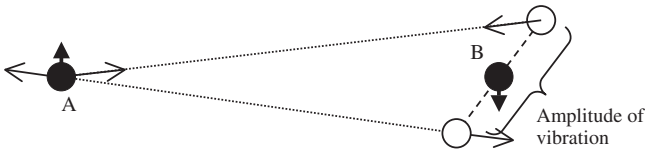

Figure 5. The bond-rotation effect. When the distance between the mean position of the atoms is held constant, a net torque on a bond direction is produced by relative thermal displacements making acute/obtuse angles with the pair potential bond. →, instantaneous force; ⟶, time-averaged force.

of the two atoms but tending to restore the time-averaged true bond length to its original value.

(c) *The 'bond-rotation effect'*. When the relative motion of two atoms has components both along the bond and transverse to it, the bond-stretching and tension effects contribute simultaneously to the thermal expansion. But in addition a further mechanism operates: the time-averaged directional tension and thrust in the bond produces a net torque tending to rotate the bond direction away from the direction of relative motion (figure 5). However, this is much less important than the other two mechanisms, because different vibrational modes tend to rotate the bond in different directions. Indeed, when bond directions are determined by symmetry, as in many cubic crystals, the net effect is zero. For non-cubic solids bond rotation can occasionally be significant, as found for example in models of orthorhombic polyethylene [28].

A concise analysis of all three mechanisms is given by Bruno *et al* [28].

2.2.3. Simple structures. The effects of mechanisms (a) and (b) are seen most simply in crystals whose symmetry allows only one distance parameter—say the nearest neighbour distance. Both mechanisms occur simultaneously with *opposite* effects. What circumstances favour mechanism (b), so that negative expansion occurs? This question was answered by Blackman [29], after a detailed study of the elasticity and low temperature thermal expansion of models for ionic crystals with the rock-salt and zinc-blende structures. 'Negative volume expansion coefficients are to be expected from open structures rather than close-packed ones, and those with relatively low shear moduli will be favoured'. This is readily understood. To reduce the positive contributions of mechanism (a), most of the excited vibrations must include only small or zero components of relative motion along bond directions. This cannot be achieved in a close-packed structure, but becomes easier for lower coordination. Moreover, such vibrations scarcely bring into play the strong bond-stretching force constants, and so have relatively low frequencies, with thresholds for excitation at correspondingly low temperatures; in contrast, most modes favouring mechanism (a) are not excited until higher temperatures. We can thus expect γ to fall at low temperatures are reached, further favouring negative expansion in this region. In the limit as $T \rightarrow 0$ only long wavelength acoustic modes are excited, and low shear moduli indicate correspondingly low frequencies for the transverse acoustic modes.

These considerations apply directly to models in which central (two-body) forces between nearest neighbours are dominant. But additional forces are needed for open structures to be stable, provided by short range non-central forces or by interactions between further neighbours. In simple structures such forces will *reduce* the tension effect: they resist vibrations transverse to bond directions, increase their frequencies and lower their amplitudes. Negative expansion will therefore be favoured when such forces are small, even though they are large enough to stabilize the open structure. Pronounced negative expansion thus may

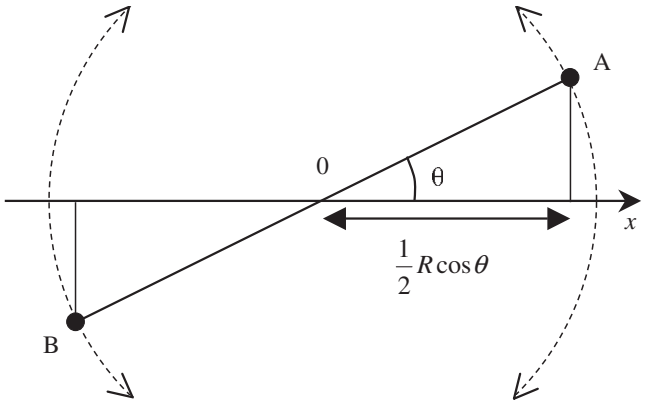

Figure 6. Libration of a bond of fixed length R reduces the distance between the mean positions of atoms A and B.

indicate that the material is close to structural instability. Recently Sikka [30] has reviewed the relation to pressure-induced amorphization.

2.2.4. Complex structures. In more complex crystals there may be several competing vibrational mechanisms contributing to the thermal expansion. There is usually more than one independent distance parameter, and more than one type of nearest neighbour bond. Moreover, unless the positions of atoms within the unit cell are fixed by symmetry, bond angles can vary with temperature. The influence of non-central forces is less obvious, because there may be cooperative motions that do not bring them into play. In general, interpretation of experimental results is difficult without good theoretical models.

2.2.5. Rigid bonds and framework structures. Interpretation is of course easier when only one or two mechanisms dominate. For example, bonds between some pairs of atoms may be so strong that they are effectively rigid. Relative motion of the atoms along the bond direction is then prohibited, and so there are no 'bond-stretching' and no 'bond-rotation' effects. But even in this limit the tension effect of figure 4 still operates[7] [31], because relative motion transverse to the bond occurs when the bond librates. Figure 6 shows a rigid bond of length R librating about the direction Ox. The mean positions of the atoms A and B remain on the Ox axis, and are given by the thermal averages

$$\langle x\rangle_T = \pm\tfrac{1}{2}R\langle\cos\theta\rangle_T \approx \pm\tfrac{1}{2}R(1-\tfrac{1}{2}\langle\theta^2\rangle_T) \tag{13}$$

where θ is the displacement of the bond from its mean orientation. Thus although the true bond length is fixed, the apparent bond length given by a diffraction measurement is reduced by a factor $\langle\cos\theta\rangle_T$, and so decreases as librational amplitudes rise with temperature. It has long been recognized that this mechanism is responsible for the negative expansion of some crystalline polymers along the chain direction. More recently the theory has been extended to materials with 'framework structures' consisting of more or less rigid groups of several atoms (usually tetrahedra or octahedra). Some of these permit low frequency vibrations involving rotations of the 'rigid units', giving rise to marked negative expansion (see below). In other

[7] For some structures one or more of the elastic stiffnesses may become infinite, raising interesting questions about the precise nature of the vibrations in this limit (see [31]).

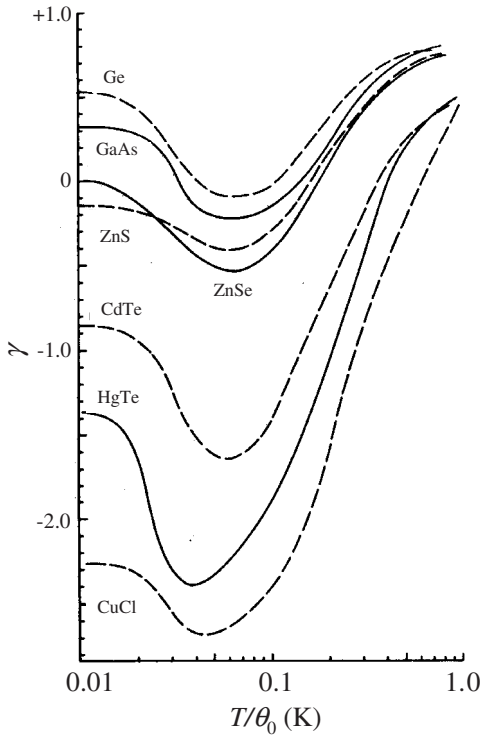

Figure 7. $\gamma(T)$ versus reduced temperature (see the text) for a range of crystals with the zinc-blende structure. The data are taken from figure 5.10 of [9].

structures, apparently closely similar, such vibrations cannot occur. Moreover, because the neighbouring rigid units are connected to each other only through a shared atom or a linking bond, it may be possible for their mean orientations to change with temperature, providing an additional mechanism for thermal expansion. For example, this second mechanism dominates in the low temperature (α) form of quartz, causing the expansion to be positive; in the high temperature (β) form the mechanism is forbidden, and the expansion becomes negative (section 3.3.6).

2.3. Examples

Because of the tension effect, negative volumetric expansion is most likely to be found in materials of open structure where coordination numbers Z are small. The following examples are taken in order of decreasing coordination number, and also of increasing complexity.

2.3.1. Alkali halides. Since negative expansion due to vibrational mechanisms is not found experimentally in materials of close-packed ($Z = 12$) and body-centred cubic ($Z = 8$) structures, we start with $Z = 6$, in a class of very well known compounds—alkali halides with the rock-salt structure. The limiting values of their Grüneisen functions at high temperatures, γ_∞, are all about 1.5, but at lower temperatures they divide into four well marked groups, interestingly determined by the cation and not the anion (see [9], figure 5.5 and table 5.2). For Li^+ salts γ alters little, but for the others it falls, to around 1.0 for Na^+, 0.35 for K^+ and -0.1 for Rb^+. Only for RbBr and RbI does the expansion become negative, and then only below

about 8 K. Nevertheless, the alkali halides are important in illustrating the general conditions for negative expansion outlined above. For lithium salts there are quite strong non-central forces, as revealed by the breakdown of the Cauchy relation $c_{12} = c_{44}$ for the elastic stiffnesses; and also the small size of the cation enhances second-neighbour interaction between anions. For these salts there is no drop in γ at low temperatures. For the other halides a steady trend towards smaller and ultimately negative values is seen as the cation becomes larger. Negative expansion is not observed in alkali halides that adopt the less open caesium chloride structure, nor in various other crystals with the rock-salt structure (e.g., MgO, PbSe).

2.3.2. Tetrahedrally coordinated structures. In the fluorite structure $Z = 4$ for the anion but $Z = 8$ for the cation. The values of $\gamma\,(T)$ for the group 2 fluorides which adopt this structure (e.g., figure 5.6 of [9]) are similar to those of the alkali halides, but none become negative; at low temperatures γ falls from γ_∞ ($\approx$1.5) to about 1.0 for CaF_2, 0.7 for SrF_2 and 0.3 for BaF_2.

For negative expansion, *both* types of atom must be tetrahedrally coordinated, as in the important series of semiconductors with the diamond, zinc-blende or wurzite structure. Figure 7 shows Grüneisen functions for several such solids plotted against reduced temperature T/Θ_0, where Θ_0 is the value of the Debye equivalent temperature for the heat capacity, $\Theta^C(T)$, as $T \to 0$ (e.g. [14, p 20]). The negative expansion is more marked and extends to higher temperatures for crystals in which the charge separation is large and there is more ionic character. For CuCl, which is the most ionic of the systems according to the Phillips ionicity factor [32] ($f_i = 0.75$), the value of β reaches a minimum of $\approx -8 \times 10^{-6}$ K^{-1} at 60 K, and does not become positive until 100 K is reached. Conversely, in diamond itself there is no charge separation, the covalent bonding is very strong and the expansion remains positive at all temperatures. At high temperatures none of these compounds has negative expansion, although for many of them β is small because of their low γ_∞ and low compressibility.

2.3.3. Cuprite structure (Cu_2O and Ag_2O). We next turn to structures containing bridging atoms with $Z = 2$. Cuprite [33, 34] has a remarkable structure, which can be visualized as two interpenetrating networks. In each network the O atoms form a diamond structure and are linked by bridging Cu atoms midway between them. There are no Cu–O bonds linking the two networks. Altogether, the O atoms form a body-centred cubic lattice, in which each O is linked through Cu atoms to only half of its eight neighbours in that lattice; thus $Z = 4$ for O and $Z = 2$ for Cu. β is negative below about 200 K, with a minimum value of about -3×10^{-6} K^{-1} near 75 K. The failure to obtain negative expansion at high temperatures may be due to interaction between the two networks.

Recently negative expansion has been found for Ag_2O also, over an even wider temperature range (10–450 K) [35]. Analysis of extended x-ray absorption fine structure [36] confirms the tension mechanism: although the mean Ag–O true bond length increases with temperature, the mean Ag–Ag nearest neighbour distance decreases in rough consistency with the bulk negative expansion. Further analysis based on a crude model suggests that the OAg_4 tetrahedra distort as well as expand on heating.

2.3.4. Bridging oxygens: RUMs and QRUMs. Despite the counter-examples of Cu_2O and Ag_2O above, negative thermal expansion in oxides is most commonly observed in crystals and glasses with strong M–O–M bridges, and is then due to the transverse vibrations of the oxygen atoms. But many oxides with M–O–M bridges do not show negative expansion. Behaviour varies because resistance to motion transverse to the bonds depends upon the details of the surrounding network as well as upon the nature of the bridge itself. For some structures there

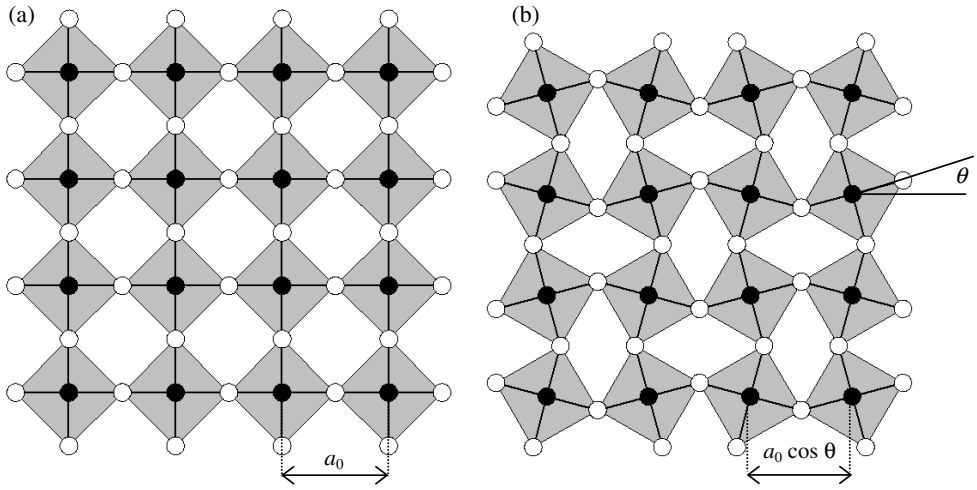

Figure 8. (a) A square lattice of rigid MO_4 units. Full circles, M; empty circles, O. (b) Rotational displacements in the lattice shown in (a), illustrating (i) a RUM, (ii) a static lattice with a bent M–O–M angle $\pi - 2\theta$.

are many modes of low frequency having strongly negative γ_j, while for others with apparently similar bonding there are not. Furthermore in many structures the oxygen sites are not wholly determined by symmetry, so mean oxygen angles may vary with temperature.

Each solid thus must be considered separately. A valuable (though oversimplified) model developed for this purpose [37] is based on the recognition that many of these materials are built up of *more or less* rigid polyhedra (SiO_4, WO_4, ZrO_6 etc) linked at their corners by shared oxygens. Large amplitude transverse vibrations of the oxygens can then occur only through coupled librations of the tetrahedra and octahedra forming the structure. Such vibrations are termed *rigid unit modes* or RUMs [38]. They involve no changes in intra-unit bond distances and angles, and so have relatively large amplitudes and low frequencies. The concept is illustrated by the 2D square lattice shown in figure 8(a), where rigid MO_4 squares are hinged to their neighbours by shared O atoms. Figure 8(b) shows a possible RUM, in which neighbouring squares librate in opposite directions. The librations reduce the lattice parameter by a factor $1 - \frac{1}{2}\langle\theta^2\rangle_T$, as in equation (13).

This approach has been developed extensively by Dove, Heine and others at Cambridge [37–42] and related to the standard Grüneisen theory. Detailed analysis is needed to find out whether a given structure can support RUMs and, if so, of what type. In some materials (e.g., ZrW_2O_8) there are large families of RUMs. In some others (e.g., ZrV_2O_7) there are no RUMs, but there are many vibrations involving libration with only small distortions of the polyhedra. These are termed *quasi-rigid unit modes* (QRUMs), and can also give rise to negative expansion. In other structures neither RUMs nor QRUMs can occur, and large negative expansion is unlikely. These concepts have helped greatly in our understanding of the expansion of framework structures, but they should not be applied uncritically. For example, in detailed lattice dynamical calculations on a rigid ion model of $AlPO_4$-17, Tao and Sleight [43] found that although RUMs contributed to negative expansion, there were many more other low frequency modes that contributed equally.

The 2D model can also be used to illustrate the change of mean oxygen angles with temperature. Suppose now that figure 8(b) represents an *equilibrium* structure in which the

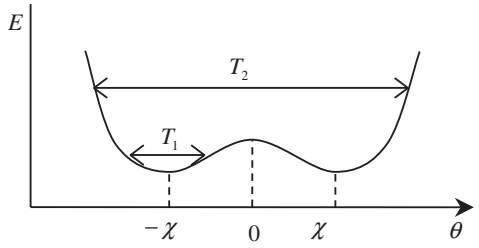

Figure 9. The static energy $E(\theta)$ of a crystal with bent oxygen angles $\pi - 2\theta$, with minima at $\theta = \pm\chi$.

oxygen angles are permanently bent, with the result that the static energy E is a minimum when $\theta = \pm\chi$ (figure 9). At low temperatures the mean structure will be close to one of the static minima, but as the vibrational amplitudes increase with temperature, $\langle\theta\rangle_T$ moves towards zero. At each temperature the librations are about a non-vanishing $\langle\theta\rangle_T$. Thus $\theta = \langle\theta\rangle_T + \varepsilon$, where $\langle\varepsilon\rangle_T = 0$. As in the previous model, the lattice parameter is proportional to $\langle\cos\theta\rangle_T$, but now

$$\begin{aligned}\langle\cos\theta\rangle_T &= \langle\cos(\langle\theta\rangle_T + \varepsilon)\rangle_T \\ &= \cos\langle\theta\rangle_T \langle\cos\varepsilon\rangle_T - \sin\langle\theta\rangle_T \langle\sin\varepsilon\rangle_T \\ &\approx \cos\langle\theta\rangle_T \left\{1 - \tfrac{1}{2}\langle\varepsilon^2\rangle_T\right\} - 0. \end{aligned} \tag{14}$$

We still have a contraction factor $\left\{1 - \frac{1}{2}\langle\varepsilon^2\rangle_T\right\}$, but the additional factor $\cos\langle\theta\rangle_T$ increases with temperature; this usually dominates, giving net positive expansion. At some higher temperature, T_c, the vibrations surmount the energy barrier and $\langle\theta\rangle_T$ becomes zero, marking a phase transition to a state where only the contraction factor remains. Thus the expansion is positive at low temperatures, due to the opening out of the mean oxygen angle, but becomes negative above a phase transition to a more symmetrical structure. In real materials the mechanisms of transition and the thermodynamic behaviour close to T_c are often difficult to determine.

2.3.5. Cubic ZrW_2O_8 and similar crystals. Cubic zirconium tungstate is the best known example of large isotropic negative expansion persisting over a wide temperature range. Although thermodynamically stable with respect to ZrO_2 and WO_3 only at high temperatures (≈1380–1500 K), it can be quenched and is then metastable from the lowest temperatures up to about 1050 K. Over all this range β is negative. The crystal is cubic[8], with a rather complex structure (figure 10): WO_4 tetrahedra and ZrO_6 octahedra are linked such that each ZrO_6 unit shares its corners with six different WO_4 units, while each WO_4 unit shares only three of its corners with ZrO_6 units; the remaining oxygen in each WO_4 tetrahedron is formally singly coordinated. The existence of terminal oxygens enhances flexibility, and theoretical analysis [37, 39] reveals families of RUMs and QRUMs of high amplitude and low frequency—a result confirmed by elastic and inelastic neutron scattering [44, 45], heat capacity [46] and other measurements. The mechanism for negative expansion has been further investigated by means of quasi-harmonic lattice dynamics [47], high pressure Raman spectroscopy [48] and x-ray absorption fine structure [49]. The elastic stiffnesses depend very strongly on temperature [50].

The lattice parameter has been determined between 2 and 520 K by high resolution powder diffractometry [51], in substantial agreement with other diffraction measurements [1, 2, 44] and

[8] A high pressure orthorhombic phase is discussed in section 3.3.8.

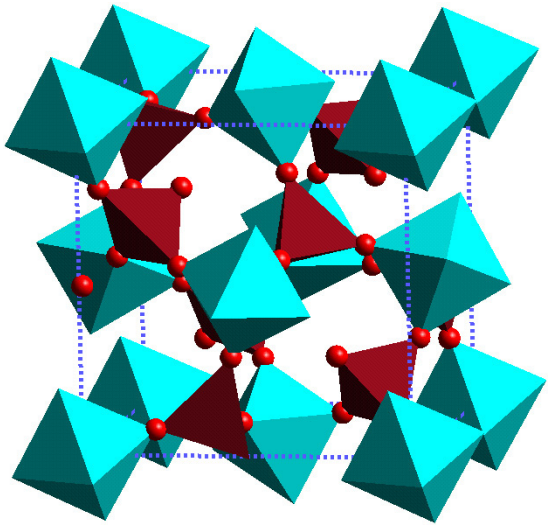

Figure 10. The room temperature structure of ZrW_2O_8. ZrO_6 octahedra (light grey) and WO_4 tetrahedra (darker grey) are shown. The spheres are oxygen atoms.

(This figure is in colour only in the electronic version)

consistently with less precise dilatometric measurements [1] extending from room temperature up to the metastability limit of 1050 K. Throughout this metastable range the thermal expansion is negative down to at least 15 K, and there is some evidence that it remains negative below this temperature. Above 50 K the volumetric coefficient $\beta \approx -27 \times 10^{-6}$ K^{-1} up to about 350 K. Between about 350 and 400 K there is a sluggish transition to a disordered but still cubic structure (β-phase); the 'terminal' oxygen atom in a WO_4 tetrahedron can migrate to another tetrahedron, thereby reversing the direction in which a pair of tetrahedra point. Above 450 K, the expansion is still negative but smaller in magnitude ($\beta \approx -13 \times 10^{-6}$ K^{-1}), presumably because the disordered structure reduces the number of RUMs and QRUMs. This behaviour continues up to 1050 K, and can be extrapolated smoothly to an isolated measurement [4] of the lattice parameter in the stable range at 1443 K.

The expansion of cubic HfW_2O_8 is essentially identical [1]. Negative expansion has also been found in crystals of similar structure with composition $ZrMo_2O_8$ [52], $Zr_{1-x}Hf_xW_2O_8$ and $ZrW_{2-x}Mo_xO_8$ [4], and $Zr_{1-x}M_xW_2O_{8-y}$ (M = Sc, In, Y) [53].

2.3.6. Cubic AM_2O_7 (A = Th, Zr, Hf, Sn; M = P, V). For many AM_2O_7 compounds the structure is again cubic. It is closely related to that of ZrW_2O_8, but each pair of unlinked tetrahedra in the ZrW_2O_8 structure is replaced by a M_2O_7 unit in which the two MO_4 tetrahedra are linked by a common oxygen. The higher coordination has been found to allow some QRUMs, but no RUMs [37].

In detail the structure is more complex than for ZrW_2O_8, involving coupled 3D rotation of slightly distorted polyhedral units and non-linear M–O–M bridges [4]. It is therefore somewhat analogous to the second 2D model discussed above: as the temperature increases mean oxygen angles may open up, causing positive expansion until a higher symmetry state is reached. Both low and high temperature forms have cubic symmetry, but at high temperatures the lattice parameter is reduced by a factor of 1/3, increasing both translational and rotational symmetry.

Behaviour varies greatly within the family. For ZrV_2O_7 it is roughly as the 2D model predicts: strong positive expansion up to about 375 K, and a small negative expansion at higher temperatures, presumably due to the QRUMs. The phase transition itself is complex, with an intermediate incommensurate structure above 345 K. For ZrP_2O_7, the transition appears simpler and occurs at about 550 K; above this the thermal expansion is weakly positive. For some of the solid solutions $ZrV_{2-X}P_XO_7$, different behaviour is found: in the middle range of x the transition disappears, and the expansion is very small and positive at room temperature, becoming negative at higher temperatures [54].

Evans [4] has measured the effective rms displacement of the oxygen atoms in ZrV_2O_7 from their ideal symmetrical sites as a function of temperature. It falls with increasing temperature up to 375 K, confirming the role of opening oxygen angles in promoting the positive expansion in this range. Above 375 K there is a normal rise in rms displacement due to increasing vibrational amplitudes, causing the observed small negative expansion.

Negative expansion at high pressures has been observed for three other members of this family, ThP_2O_7, UP_2O_7 and HfV_2O_7 [55, 56]. Interestingly, two members for which this is not so, TiP_2O_7 and ZrP_2O_7, are stable under pressure, while ZrV_2O_7 is not [57]—a further association of negative expansion with near instability.

2.3.7. Silica and zeolites. *Cristobalite* is a cubic form of silica, and consists of a network of SiO_4 tetrahedra linked to each other by shared oxygens. Despite its open structure, the expansion of the low temperature (α) phase is strongly positive due to the opening of Si–O–Si angles; but in the high temperature (β) phase this mechanism is forbidden, and the expansion is very small, or even negative. At these temperatures the vibrations are strongly anharmonic; the behaviour has been successfully simulated by molecular dynamics [58]. Small negative expansion has also been observed above 1100 K for the cristobalite form of $AlPO_4$ [59].

Zeolites are microporous solids with open framework structures. Most of them are aluminosilicates with additional positive ions, but some can be formed from pure silica. In a seminal paper Couves *et al* [60] reported lattice dynamical simulations by Parker and Tschaufeser (see also [61]) for three cubic materials. Two were pure silica, each formed from 'β-cages' of 24 Si atoms bound by O links: in sodalite the cages are fixed together with Si atoms in common; in siliceous faujasite (a zeolite) the cages are linked by oxygen bridges, forming a more open structure. The simulations predicted positive expansion for sodalite, as expected; but for the faujasite negative expansion ($\alpha \approx -4 \times 10^{-6}$ K^{-1}) was found over the whole range between 50 and 500 K, and smaller but appreciable negative expansion for the aluminosilicate Na–zeolite X. These predictions were subsequently confirmed by powder diffraction measurements for sodalite and Na–zeolite X [60], and later for siliceous faujasite [62]. For non-cubic zeolites see section 3.3.7.

2.3.8. Glasses and glass ceramics. The expansion of these materials has been reviewed by White (e.g. sections 5.8 and 5.9 of [9], 5.4 of [14]). It depends on preparation and ageing. Pure vitreous silica has a lower density than crystalline forms, and expansion is negative below about 150 K, with γ falling to about -6 at low temperatures. The negative expansion can be reduced by increasing the density slightly, via heat or irradiation. Additives that are network *fillers*, such as Na_2O or K_2O, also reduce the negative expansion. TiO_2, a network *replacer*, enhances the negative expansion at low temperatures and leads to near-zero expansion at room temperatures; this is the basis of one ultralow expansion glass (Corning ULE). Molecular dynamics simulations indicate that the negative expansion of silica glass is also enhanced by pressure [63]. For some other tetrahedrally bonded glasses also the expansion is negative at

low temperatures, whereas for non-tetrahedrally bonded glasses (including polymeric ones) it has been found to be positive (except below about 1 K).

In many glasses the heat capacity has been found not to fall off as T^3 at the lowest temperatures (as predicted by the Debye theory) but below 1 or 2 K to become dominated by a term closely linear in T which persists down to the mK region. The thermal expansion in this range is too small to measure with current techniques, but measurements above 1 K indicated (from extrapolation of plots of α/T against T^2) values for α/T of about -0.5×10^{-9} K^{-2} for various silica glasses and -3.5×10^{-9} K^{-2} for the polymeric PMMA glass, each corresponding to Grüneisen parameters of about -16 (see also [9]). Later measurements extending below 1 K indicated a much smaller linear term for PMMA giving a Grüneisen parameter of about -1 (see [14]). It has been postulated [64, 65] that the 'linear term' is due to the presence of tunnelling systems (see section 4.1.2) with a wide distribution of energy splittings, or alternatively to the vibrational frequency distribution of a highly disordered system [66, 42]. Further work is required.

Glass ceramics are important technical materials that are formed in the glassy state and then partially crystallized to give high mechanical strength with zero porosity, with thermal expansion depending crucially on composition. Generally the addition of $LiAlO_2$ to silica leads to strong negative expansion (see also section 3.3.10).

3. Anisotropic materials

3.1. Introduction

The volumetric expansion coefficient β can of course be negative in non-cubic as well as in cubic materials. Even when β is positive, one or two of the three principal linear coefficients may be negative. The variety of behaviour is thus even richer than for cubic materials; but underlying mechanisms are similar. The hexagonal crystal graphite provides a particularly simple example [67]. The coefficient of expansion perpendicular to the axis, $\alpha_\perp$, is negative over a wide range below room temperature, while the expansion parallel to the axis, $\alpha_\parallel$, is positive (figure 11). This is to be expected from the structure, which is built up from layers of carbon atoms tightly bound in planar honeycomb layers; between the layers there are only weak dispersion forces. The crystal is therefore highly compressible along the hexagonal axis, but very stiff in directions normal to the axis. Those vibrational modes with atomic motions polarized parallel to the axis (and so normal to the strong intraplanar forces) have *low* frequencies and *large* amplitudes, while those polarized perpendicular to the axis have relatively *high* frequencies and *small* amplitudes. At low temperatures, the low frequency modes are preferentially excited, producing compressive thermal stress normal to the planes (the bond-stretching effect) and comparable tensile stress within the planes (the tension effect). However, the magnitude of the consequent negative $\alpha_\perp$ is much smaller than that of the positive $\alpha_\parallel$, because of the much greater stiffness within the planes than between them. At high temperatures, vibrations polarized perpendicular to the axis become more fully excited and contribute additional compressive stress within the planes, so $\alpha_\perp$ becomes positive.

This interpretation of the expansion of graphite in terms of bond-stretching and tension effects is based on the concept of pair potentials. Pair potential models of simple structures, including loosely bound plain layers [68], coupled chains [68] and loosely bound chains [69], have shown how behaviour depends on structure and bonding; for most models (not all) any negative expansion occurs in elastically stiff directions below room temperature. But pair potential models cannot approach the complexity in structure and bonding of many materials. Before considering real materials in detail, we extend the thermodynamics of section 2.1 to non-cubic crystals.

3.2. Thermodynamics; quasi-harmonic theory

To describe changes of shape as well as volume, we need to specify at least two independent parameters, called *strains*, with their thermodynamically conjugate *stresses*. In any non-cubic material, changing the temperature at fixed strain causes anisotropic thermal stress; the resulting expansion is then determined by the elasticity of the material, which also is anisotropic. A general analysis, applicable to materials of any symmetry under arbitrary stress, is well established [70–73]. Here we give a simpler analysis dealing only with materials of orthorhombic or higher symmetry, expanding at zero pressure.

In an orthorhombic crystal there are three independent dimensions a, b, c along the three principal axes. Strain coordinates η_λ are defined such that

$$\mathrm{d}\eta_1 = \mathrm{d}\ln a, \qquad \mathrm{d}\eta_2 = \mathrm{d}\ln b, \qquad \mathrm{d}\eta_3 = \mathrm{d}\ln c. \tag{15}$$

The expansion coefficients $\alpha_\lambda = (\partial\eta_\lambda/\partial T)_P$ are

$$\begin{aligned} &\alpha_1 = \alpha_a = (\partial \ln a/\partial T)_P, \qquad \alpha_2 = \alpha_b = (\partial \ln b/\partial T)_P, \\ &\alpha_3 = \alpha_c = (\partial \ln c/\partial T)_P. \end{aligned} \tag{16}$$

The three independent stresses σ_λ conjugate to the strains are defined by

$$\sigma_\lambda = (1/V)\,(\partial F/\partial\eta_\lambda)_{\eta',T} \tag{17}$$

where the subscript η' denotes that all other strains are kept constant. The σ_λ have the dimensions of pressure, but are *tensile* stresses; for example, under isotropic pressure $\sigma_1 = \sigma_2 = \sigma_3 = -P$. As in equation (5), the thermal stress coefficients are related to dimensionless Grüneisen functions γ_λ:

$$\left(\frac{\partial\sigma_\lambda}{\partial T}\right)_\eta = -\frac{C_\eta}{V}\gamma_\lambda, \qquad \gamma_\lambda = -\left(\frac{\partial\sigma_\lambda}{\partial(U/V)}\right)_\eta \tag{18}$$

where C_η is the heat capacity at constant strain; the negative signs arise because σ_λ refers to tensile stress. The Grüneisen functions may be written as either γ_1, γ_2, γ_3 or γ_a, γ_b, γ_c.

As Munn [74] has emphasized, the elastic response to the thermally generated stress is more complex than for isotropic solids; in particular, the signs of α_λ and γ_λ are not necessarily the same, because a stress applied in one direction affects the dimensions in all three directions. Elastic response to stress is described by a matrix of isothermal or adiabatic *compliances*, $s^T_{\lambda\mu}$ or $s^S_{\lambda\mu}$, which together form a generalization of the compressibility:

$$s^T_{\lambda\mu} = \left(\frac{\partial\eta_\lambda}{\partial\sigma_\mu}\right)_{\sigma',T}, \qquad s^S_{\lambda\mu} = \left(\frac{\partial\eta_\lambda}{\partial\sigma_\mu}\right)_{\sigma',S}. \tag{19}$$

Expansion coefficients are then given by analogues of equation (6):

$$\alpha_1 = \frac{C_\eta}{V}\left(s^T_{11}\gamma_1 + s^T_{12}\gamma_2 + s^T_{13}\gamma_3\right) = \frac{C_P}{V}\left(s^S_{11}\gamma_1 + s^S_{12}\gamma_2 + s^S_{13}\gamma_3\right), \text{ etc.} \tag{20}$$

While the *direct compliances* s_{11}, s_{22} and s_{33} are always positive, the *cross-compliances* s_{12}, s_{23} and s_{13} are usually negative, and so applying a tension in one direction causes extension in that direction but contraction in the other directions (Poisson's ratio is usually positive). Negative thermal expansion can therefore sometimes occur even when *all* the γ_λ are positive.

Materials of 'axial' symmetry (tetragonal, hexagonal, trigonal and cylindrical) have only two independent dimensions: c along the main symmetry axis and a perpendicular to it. The independent expansion coefficients are then (in various common notational forms)

$$\alpha_\perp = \alpha_a = \alpha_1 = \alpha_2 = (\partial \ln a/\partial \ln T)_P, \qquad \alpha_\parallel = \alpha_c = \alpha_3 = (\partial \ln c/\partial \ln T)_P \tag{21}$$

and the Grüneisen functions are

$$\begin{aligned}\gamma_\perp = \gamma_a = \gamma_1 = \gamma_2 &= -\left(\frac{\partial\sigma_1}{\partial(U/V)}\right)_\eta = \frac{1}{2}\frac{(\partial S/\partial \ln a)_{T,c}}{C_\eta} \\ \gamma_\parallel = \gamma_c = \gamma_3 &= -\left(\frac{\partial\sigma_3}{\partial(U/V)}\right)_\eta = \frac{(\partial S/\partial \ln c)_{T,a}}{C_\eta}.\end{aligned} \tag{22}$$

Equation (20) reduces to

$$\begin{aligned}\alpha_\perp &= \frac{C_\eta}{V}\left\{(s_{11}^T + s_{12}^T)\gamma_\perp + s_{13}^T\gamma_\parallel\right\} = \frac{C_P}{V}\left\{(s_{11}^S + s_{12}^S)\gamma_\perp + s_{13}^S\gamma_\parallel\right\} \\ \alpha_\parallel &= \frac{C_\eta}{V}\left\{2s_{13}^T\gamma_\perp + s_{33}^T\gamma_\parallel\right\} = \frac{C_P}{V}\left\{2s_{13}^S\gamma_\perp + s_{33}^S\gamma_\parallel\right\}.\end{aligned} \tag{23}$$

Munn [74] has also expressed these relationships in terms of the directional compressibilities

$$\chi_\perp = s_{11} + s_{12} + s_{13} \qquad \chi_\parallel = 2s_{13} + s_{33} \tag{24}$$

so as to show more clearly the respective parts played by anisotropy in the elasticity and in the γ_λ:

$$\begin{aligned}\alpha_\perp &= \frac{C_P}{V}\left\{\chi_\perp^S\gamma_\perp + s_{13}^S(\gamma_\parallel - \gamma_\perp)\right\} \\ \alpha_\parallel &= \frac{C_P}{V}\left\{\chi_\parallel^S\gamma_\parallel - 2s_{13}^S(\gamma_\parallel - \gamma_\perp)\right\}\end{aligned} \tag{25}$$

which may be compared with equation (6). When the Grüneisen functions are isotropic ($\gamma_\parallel = \gamma_\perp$) the thermal expansion has the anisotropy of the directional compressibilities. Otherwise, the further terms in $\gamma_\parallel - \gamma_\perp$ are important unless s_{13} is small.

3.2.1. Quasi-harmonic theory. The extension of quasi-harmonic theory to anisotropic materials is straightforward. For details, see e.g. [9, 14, 21, 71, 75].

3.3. Examples

The elasticity of most materials is determined mainly by the static lattice energy function, and varies comparatively little with temperature. It is then a good first approximation to treat the compliances $s_{\lambda\mu}$ as constant, and regard the temperature dependence of the thermal expansion as due solely to that of the heat capacity and the γ_λ. Room temperature elastic coefficients are tabulated in the Landolt–Börnstein series [76]. Table 1 lists relevant compliances for a selection of materials of axial symmetry that are discussed below. They exemplify different types of structure and bonding, but all have negative expansion in at least one direction.

3.3.1. Wurzite structure and hexagonal ice. These hexagonal crystals have tetrahedral coordination similar to that of the cubic zinc-blende structure, and like them may have negative expansion over wide ranges below room temperature, sometimes with considerable anisotropy.

For *zinc oxide* [77, 78] β is negative until above 100 K, and γ falls to about -1.1 as $T \to 0$. Because s_{13} is large and negative, a small anisotropy in γ_λ is greatly magnified in α_λ: $\alpha_\parallel$ reaches a minimum of -0.9×10^{-6} K^{-1} at about 70 K and stays negative until about 127 K is reached, while $\alpha_\perp$ reaches only -0.5×10^{-6} K^{-1} at about 60 K, and stays negative until about 99 K is reached. For details and for other wurzite structure crystals (including AgI, for which $\alpha_\parallel$ reaches -12×10^{-6} K^{-1} at 20 K), see sections 5.6.2 of [9] and 5.5.2 of [14].

In *hexagonal ice*, hydrogen bonds form a tetrahedral linkage of oxygen atoms. Anisotropy is weak, and $\alpha_\parallel$ and $\alpha_\perp$ both become negative below about 60 K [79].

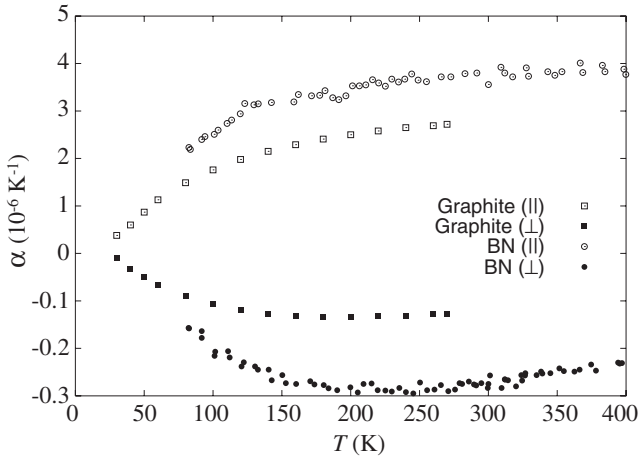

Figure 11. Linear expansion coefficients of pyrolytic graphite [67] and hexagonal boron nitride [82]. The scale for the positive $\alpha_\parallel$ is ten times that for the negative $\alpha_\perp$. The data are taken from figure 5.19 of [9].

Table 1. Room temperature elastic compliances in $(\text{TPa})^{-1}$ for selected materials [76].

	s_{11}	s_{12}	$s_{11}+s_{12}$	s_{33}	s_{13}	$\chi_\perp$	$\chi_\parallel$
Graphite	0.98	−0.16	0.82	27.5	−0.33	0.49	26.8
ZnO	7.82	−3.45	4.37	6.64	−2.10	2.27	2.44
Ice (250 K)	105	−40	65	87	−25	40	37
α-As	30.6	20.5	51.1	140	−56	−4.9	28
InBi	52.9	−18.3	34.6	88.3	−32.1	2.5	24.1
Zn	8.22	0.60	8.82	27.7	−7.0	1.22	13.7
Cd	12.2	−1.2	11.0	33.8	−8.9	2.1	16.0
Se	131	−13	118	41	−40	78	−39
Te	53.4	−16.1	37.3	24.3	−13.6	23.7	−2.9

3.3.2. Layered structures. In an ideal layered crystal, strongly bonded two-dimensional arrays are bound to each other much more weakly in the third direction (the c direction for axial crystals). It is difficult to deform the layers in the a and b directions, and so s_{11} and the cross-compliances s_{12} and s_{13} are much smaller than s_{33}. In table 1, graphite approximates these conditions quite closely, while α-As, Zn, Cd and InBi have some layered characteristics but are far from ideal.

Our earlier qualitative discussion of *graphite* neglected the effect of the small cross-compliance s_{13}. Although much smaller than s_{33}, it is of the same order as $s_{11}+s_{12}$ and significantly affects $\alpha_\perp$. Measurements on pyrolytic graphite [67] show that $\gamma_\perp$ is about −5.3 at 40 K, rising to about −1 at 273 K, while $\gamma_\parallel$ is about 3.4 at 40 K, falling to about 0.8 at 273 K. The negative $\alpha_\perp$ is due primarily to the tension effect within the layers (negative $\gamma_\perp$), but because s_{13} is negative it is enhanced by the positive thermal pressure between the planes[9] [80]. $\alpha_\perp$ continues to be negative well above room temperature, becoming positive at about 650 K [81]. *Hexagonal boron nitride* behaves similarly [82] (figure 11).

α-arsenic is another elemental crystal for which $\alpha_\perp$ is negative below room temperature [83]. As in graphite, each atom is tightly bound to three neighbours, but the bonds

[9] Earlier theory [80] neglected the tension effect and ascribed the negative expansion solely to the cross-compliance.

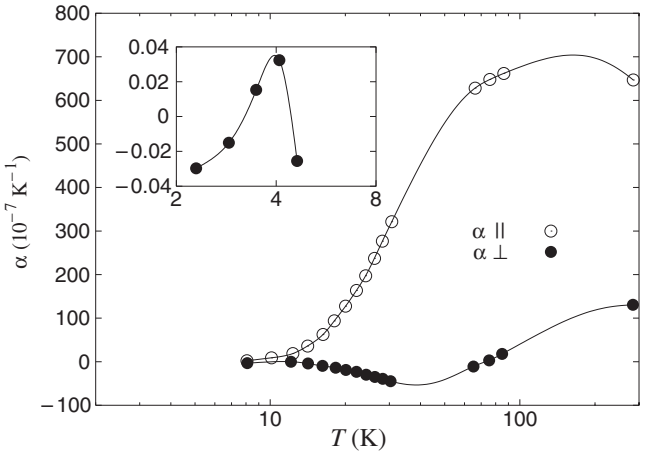

Figure 12. Linear expansion coefficients of zinc. The inset shows the very low temperature behaviour of $\alpha_\perp$. The data are taken from [71].

are no longer coplanar. They are almost at right angles to each other, so as to form strongly puckered sheets lying perpendicular to the c axis. The Grüneisen functions are positive and approximately isotropic, with values of about 4.0 at 0 K, falling to about 1.5 at 270 K as higher frequency modes become excited. $\alpha_\perp$ is negative because of the large negative s_{13}. At low temperatures, $\gamma_\perp - \gamma_\parallel$ in equation (25) is very small and so $\alpha_\perp$ has the same sign as $\chi_\perp$. By 270 K, $\gamma_\perp - \gamma_\parallel$ has increased to about 0.08, which is just sufficient to make $\alpha_\perp$ positive. Above room temperature, x-ray diffraction has shown that $\alpha_\perp$ remains close to zero up to 677 K [84].

Zinc and *cadmium* (for original measurements see [9]) provide further striking examples of the role of a large negative s_{13}. The structure is a hexagonal close-packed one, but the nearest neighbour distance within the (0001) basal planes is shorter than that between the planes, indicating stronger bonding. The 'layers' are thus planar, giving some resemblance to graphite, but with metallic bonding both within and between the layers. $\gamma_\parallel$ and $\gamma_\perp$ remain positive at all temperatures, but for both metals s_{13} drives $\alpha_\perp$ negative whenever $\gamma_\perp$ is less than $\approx 0.8\gamma_\parallel$. The oscillation of $\alpha_\perp$ below 10 K in Zn (figure 12) is a consequence [71, 85] of the temperature variation of $\gamma_\perp$ and $\gamma_\parallel$. The sharp curvature at the lowest temperatures is due to the onset of electronic effects.

With more complex structure and bonding it becomes more difficult to predict or explain the thermal expansion (see, e.g., [86] for a prediction of the thermal expansion of $MgCl_2$). In the examples above, negative expansion occurs in the elastically harder directions, and is smaller in magnitude than the positive expansion in other directions; but the semi-metal *indium bismuth*, InBi, breaks these rules. The In atoms lie in planes forming square lattices, where each atom is tetrahedrally bonded to two Bi atoms in a plane above and two in a plane below, forming corrugated triple layers. Elastically the axial direction is softer (table 1). The Grüneisen functions are both positive, but now $\gamma_\perp > \gamma_\parallel$ and the large negative s_{13} drives $\alpha_\parallel$ large and negative. At room temperature, $\alpha_\parallel = -85 \times 10^{-6}\ \mathrm{K}^{-1}$, $\alpha_\perp = 61 \times 10^{-6}\ \mathrm{K}^{-1}$. For further discussion see section 8.4.6 of [14].

3.3.3. Chain structures (e.g., crystalline polymers). Once again, the basic ideas are relatively straightforward (e.g. [69, 87]). In the simplest model (a 'bundle of rods') the chains are linear and stiff, while the binding between them is weak, so the crystal is elastically stiff only in the

parallel direction along the chains. At low temperatures, vibrations polarized along the strong bonds are excited much less than the lower frequency vibrations polarized in directions away from these bonds. In contrast to the case for simple layered crystals, but because of similar mechanisms, it is now $\gamma_\parallel$ that is negative and $\gamma_\perp$ that is positive. The thermal expansion in the stiff chain direction is thus negative but small, until the temperature is high enough to excite vibrations in the strong bonds. However, although this is a useful model, it oversimplifies the behaviour of real materials.

Trigonal selenium and tellurium provide monatomic examples of negative $\alpha_\parallel$. The chains are helical, and are arranged in a hexagonal array such that each helix has six neighbours. Thus there are two independent cell dimensions, a and c, and one internal dimension, R, the helix radius. For Se the expansion is strongly anisotropic even at room temperature [88], with $\alpha_\parallel = -13 \times 10^{-6}$ K^{-1}, $\alpha_\perp = 69 \times 10^{-6}$ K^{-1}. For Te the intrachain valence bonding is less dominant, but $\alpha_\parallel$ is still negative at room temperature: $\alpha_\parallel = -2.3 \times 10^{-6}$ K^{-1}, $\alpha_\perp = 29.5 \times 10^{-6}$ K^{-1}. X-ray measurements show that the helix radius contracts strongly with increasing temperature; $\alpha_R \approx -35 \times 10^{-6}$ K^{-1} [89]. The influence of this internal degree of freedom on the macroscopic expansion has been investigated by Gibbons in a theoretical model [90].

In those *organic crystalline polymers* where the carbon skeletons are planar, such as polyethylene, the low frequency vibrations are polarized mainly normal to the skeletal planes. They depend partly on the weak intrachain forces caused by torsional distortion of the chains and partly on interactions between the chains. Vibrations polarized along the chain depend mainly on strong intrachain forces; they are mostly of small amplitude and high frequency, and so are not excited at low and intermediate temperatures. The amplitude of the excited atomic vibrations is therefore mainly perpendicular to the chains, so the thermal expansion in the chain direction is dominated by tension effects and is negative. The interchain interaction is affected by both bond-stretching and tension effects; generally the bond-stretching effect is greater, producing positive expansion in directions perpendicular to the polymer chains. Quantitatively the behaviour can be complex, especially the anisotropic expansion normal to the chains, requiring detailed polymer-specific models and simulations (see e.g. [28] and [91] for work on crystalline polyethylene and [92] and [93] for work on other polymer crystals).

Orthorhombic polyethylene is a much studied example. The structure [94] is shown in figure 13. The planar carbon chains run continuously in the c direction. As shown in figure 14, α_c is negative, while the expansion coefficients α_a and α_b normal to the chain direction are positive, and larger by at least an order of magnitude [95, 96]. There is also a (less marked) anisotropy in the ab plane, with $\alpha_a > \alpha_b$ down to at least 100 K. The tension effect, due primarily to vibrations perpendicular to the polymer planes, is as usual responsible for the negative expansion in the chain direction: the calculated γ_c is large and negative at low temperatures, becoming much smaller at high temperatures. Bruno *et al* [28], using quasi-harmonic lattice dynamics, found that the anisotropy in the ab plane resulted from a subtle interplay of the thermal stress and the elasticity. The calculated expansion coefficients are compared with experiment in figure 14; they predict that the anisotropy of the expansion normal to the chains is greatly reduced or even reversed at low temperatures.

Lacks and Rutledge [93] have discussed the different roles played by thermal stresses and elasticity in the negative axial thermal expansion of both crystalline polyethylene and *isotactic polypropylene*.

The expansion of a well aligned sample of *polyoxymethylene* (POM, $[CH_2O]_n$) has been measured at low temperatures [97]. $\alpha_\parallel$ was negative below 100 K, with a minimum of -2.0×10^{-6} K^{-1} at 40 K.

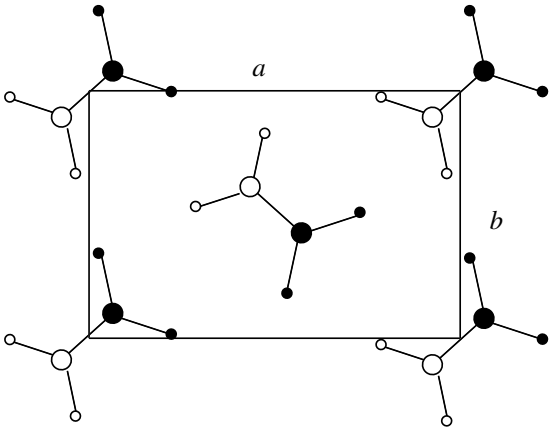

Figure 13. The unit cell of ideal orthorhombic polyethylene. $a = 7.478$ Å, $b = 4.970$ Å, $c = 2.515$ Å. Full circles denote atoms at height $c/4$; empty circles denote atoms at height $-c/4$. Large circles denote C and small circles H atoms. The data are taken from [94].

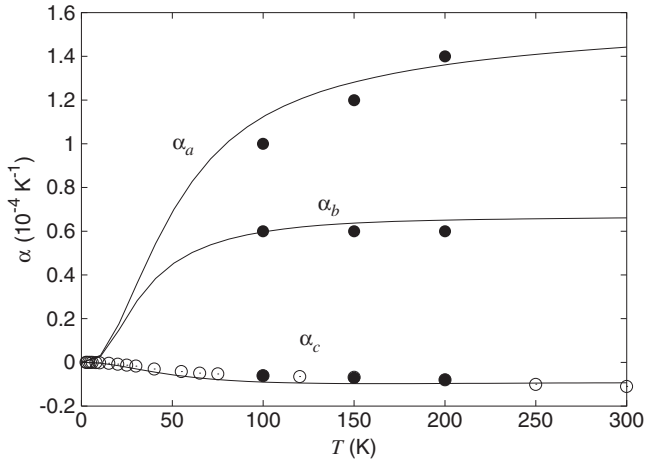

Figure 14. The thermal expansion of orthorhombic polyethylene. Experiment: ● [95]; ○ [96]. Theory: —— [28].

3.3.4. Oxides. Many non-cubic oxides that exhibit negative thermal expansion are framework structures in which there are bridging oxygen atoms. These are discussed in the following sections. But we first mention some exceptions. *Paratellurite* (TeO_2) has the tetragonal rutile structure. Although $\alpha_\parallel$ and $\alpha_\perp$ are both positive at room temperature, $\alpha_\parallel$ becomes negative [98] in the elastically dominated range below 10 K, and β below 7 K, owing to the soft stiffness $c_{11} - c_{12}$. *Hexagonal* $CuScO_2$ has the delafossite structure, where each Sc atom is octahedrally coordinated to six oxygen atoms so as to form oxygen–scandium–oxygen sandwiches piled on top of each other. The adjoining oxygen layers are bound to each other by O–Cu–O bridges parallel to the hexagonal axis. Neutron diffraction measurements [99] between liquid helium and room temperatures show a negative expansion between adjoining oxygen layers of $\approx -4 \times 10^{-6}\ \mathrm{K}^{-1}$. The net crystal expansion along the hexagonal axis, $\alpha_\parallel$, is only $-1.3 \times 10^{-6}\ \mathrm{K}^{-1}$. Above room temperature $\alpha_\parallel$ is positive. Another copper compound,

orthorhombic melanothallite (Cu_2OCl_2), has a negative expansion along one axis *above* room temperature: $\alpha_b = -26.7\times10^{-6}\,K^{-1}$. This has been interpreted as due to a 'hinge mechanism' in which the angle varies between chains of Cu_2OCl_2 squares [100].

3.3.5. Anisotropic oxides with framework structures; phenacites. Most framework structures have symmetry lower than cubic, giving anisotropic expansion. But broadly the same considerations apply to them as to cubic materials. RUMs and QRUMs may contribute negatively to thermal expansion, but now have anisotropic effects, so not only the apparent size of a polyhedron but also its apparent shape may be affected. Also, as in the model of figure 8(b), the symmetry may be low enough to permit mean oxygen angles to vary with temperature without distorting the polyhedra, resulting in positive expansion until a higher symmetry is reached.

Most of these structures are built of AO_4 tetrahedra and BO_6 octahedra, linked at the corners by two-coordinated oxygens. But the hexagonal phenacite (Be_2SiO_4) structure is built of tetrahedra linked by three-coordinated oxygens, thus forming a network that is less open than silica but more open than wurtzite. The expansion of at least two compounds with this structure is negative at low temperatures. Zn_2SiO_4 (*willemite*) has $\alpha_\parallel$ negative below room temperature, with a minimum of $\approx -2.0\times10^{-6}\,K^{-1}$ at 100 K; $\alpha_\perp$ is negative below 150 K, with a minimum of $\approx -0.9\times10^{-6}\,K^{-1}$ at 80 K [101]. Zn_2GeO_4 has recently [102] been reported to have an average α of $-3.4\times10^{-6}\,K^{-1}$ below room temperature and of $3.9\times10^{-6}\,K^{-1}$ above room temperature, indicating that it might be a useful low expansion material at ambient temperatures.

3.3.6. Quartz and similar crystals. The open structure is composed of SiO_4 tetrahedra linked by shared oxygen atoms at each corner. Below 846 K the symmetry is trigonal (α-quartz), and helical arrangements of the tetrahedra about axes in the c direction permit the mean Si–O–Si angles to change by cooperative tilting of the tetrahedra, causing positive expansion in both a and c directions over a wide temperature range [103]. But this mechanism can no longer occur (cf the 2D model in section 2.3.4) after hexagonal symmetry (β-quartz) is reached at 846 K, where there is a lambda transition. Both $\alpha_\parallel$ and $\alpha_\perp$ then fall sharply as T increases, and soon become small and negative, due presumably to the librations of the tetrahedra about their mean symmetric orientation. Neutron diffraction data [104] at 863 K indicate that just above the transition the SiO_4 tetrahedra are disordered, with dynamic switching between local symmetries of the two forms of α-quartz—a picture in accordance with more recent molecular dynamics simulations [105]. It would be interesting to relate this work to the semi-empirical RUM model of Welche *et al* [40] and to the extended lattice dynamical treatment of Smirnov [106].

Both $\alpha_\perp$ and $\alpha_\parallel$ remain positive down to 12 K; below this, $\alpha_\parallel$ becomes negative (indicating apparent tetrahedral distortion). As $T\to0$, $\gamma_\perp\to0.7$ and $\gamma_\parallel\to-0.8$. A quasi-harmonic model [107] gives qualitative agreement with this behaviour.

There are three compounds MPO_4 of similar structure to quartz, with silicon replaced alternately by M (Al, Fe or Ga) and by P. Both $FePO_4$ [108–110] and $AlPO_4$ (*berlinite*) [111] have rather similar expansion to quartz at higher temperatures, but as yet neither measurement nor theory has been extended to the very low temperatures at which $\gamma_\parallel$ becomes negative for quartz.

3.3.7. Zeolites and $AlPO_4$s. The prediction from quasi-harmonic calculations [61, 112] of strong negative expansion in several non-cubic zeolites and $AlPO_4$s was confirmed

experimentally for many different materials. This work has been reviewed up to 1999 by Lightfoot *et al* [113], who discuss also why other zeolites and $AlPO_4$s have positive expansion. Recent papers include quasi-harmonic calculations on $AlPO_4$-17 [114], and experimental measurements on pure silica zeolite IFR [115], calcined siliceous ferrierite [116] and hydrated HZSM-5 orthorhombic zeolite [117], all of which throw light on mechanisms.

3.3.8. Orthorhombic ZrW_2O_8. At pressures over 0.2 GPa, cubic ZrW_2O_8 transforms to an orthorhombic γ-phase [118, 119] with an ≈5% reduction in cell volume. The unit cell is closely related to that of the cubic phase, but the length of one axis is tripled. In this less open structure the average W and O coordination numbers are increased due to enhanced interactions between adjacent WO_4 groups; the one-coordinated oxygens in the cubic structure all become two-coordinated ones. This phase is retained when the pressure is released, and the decreased flexibility reduces the tension effect to give smaller negative expansion. Below ≈150 K the expansion is almost isotropic, with $\beta \approx -5 \times 10^{-6}$ K^{-1}. Expansion is small ($\beta \approx -1 \times 10^{-6}$ K^{-1}) at room temperature, and above 350 K it is highly anisotropic, with $(\alpha_a, \alpha_b, \alpha_c) \approx (11.5, 4.5, -10.5) \times 10^{-6}$ K^{-1}. At about 390 K the crystal reverts to the more stable cubic phase.

3.3.9. $Sc_2(WO_4)_3$ and similar crystals. Scandium tungstate is orthorhombic, with a framework structure containing WO_4 tetrahedra and ScO_6 octahedra joined at the corners; all oxygens are shared [120]. The thermal expansion is anisotropic, with α_a and α_c negative and α_b positive; $\beta = -6.5 \times 10^{-6}$ K^{-1} over the range 50–450 K, and negative expansion continues up to at least 1073 K [121]. The same general mechanisms operate as in ZrW_2O_8 and ZrW_2O_7. There are many other compounds $A_2M_3O_{12}$ which have the same crystal structure, although many of them become monoclinic at lower temperatures, with positive expansion below the phase transition temperature (e.g. 178 K for $Sc_2(MO_4)_3$ [122]). A wide range of cations can be found on the A sites, ranging in size from Al^{3+} to the smaller rare earths; M is usually Mo or W (see e.g. [123, 124] and the survey in [4]). In $Lu_2(WO_4)_3$ and $Y_2(WO_4)_3$ the cations have ionic radii of about 1 Å; α_a, α_b and α_c are all negative, and the magnitude of the negative β is three times that of $Sc(WO_4)_3$ [125, 126]. Unfortunately their hygroscopicity limits their potential use [127]. Smaller AO_6 octahedra appear to inhibit transverse oxygen vibrations. For $Al_2(WO_4)_3$ the cationic radius is about 0.53 Å; α_a and α_c are only weakly negative, and a large positive α_b leads to a positive volumetric coefficient β [126, 128, 129].

The expansion of many of these materials can be controlled by appropriate substitutions. Because of the high anisotropy, the expansion of polycrystalline samples can show hysteresis (see e.g. [130, 131] and also section 3.3.13).

3.3.10. Lithium alumina silicates. The discovery of the ultralow thermal anisotropic expansion of β-spodumene ($LiAlSi_2O_6$) [132], and subsequently of negative expansion in β-eucryptite ($LiAlSiO_4$) [133], a hexagonal derivative of β-quartz, together with their solid solutions, led to the commercial development of low expansion ceramics for dinnerware and mirror blanks for the largest telescopes. Lithium alumina silicates such as β-eucryptite dominated the market for many years and play an important role in determining the expansion coefficient of ceramic glasses. For β-eucryptite, α_c is negative above 20 K with a value of -20×10^{-6} K^{-1} at 300 K. In the *a* and *b* directions the expansion is positive, so β is close to zero over a wide temperature range. Two materials for which extensive experimental measurements exist are Cer-Vit (Owens-Illinois) and Zerodur (Schott) [134]. By careful adjustment of the chemical content and heat treatment an expansion coefficient can be achieved which is close to

zero over a desired temperature range. These very low expansion materials are crucial in the fabrication of large optical components because they retain their shape despite changes that occur both during polishing and during operation.

3.3.11. NZP and related compounds; other phosphates. Another family which has attracted wide attention since the early 1980s is the NASICON or NZP family based on the $NaZr_2(PO_4)_3$ structural type; [12] is a useful review of work up to 1989. Unlike in β-eucryptite and spodumene, very many substitutions are possible. For example, Na can be replaced by elements as diverse as Cs, Cu, H and Li. Different substitutions lead to a wide range of expansion behaviour ranging from negative expansion in $NbTi(PO_4)_3$ [135], to zero expansion in $Ca_{0.25}Sr_{0.25}Zr_2(PO_4)_3$ [136], and to large positive expansion in $Ca_{0.25}Na_{0.5}Zr_2(PO_4)_3$ [137]. NZP itself has space group $R\bar{3}c$; it contains corner-sharing ZrO_6 octahedra, each of which is connected to six PO_4 tetrahedra, while each PO_4 tetrahedron is linked to four ZrO_6 octahedra. Once again, coupled rotation of the oxygen-sharing polyhedral building blocks of this open structure has been used to account for the anisotropic expansion. α_c is generally positive and α_a negative. Substitution of a divalent ion such as Sr^{2+} or Ca^{2+} for Na^+ leads to an ordering of cations and vacancies (e.g. [138]) and the symmetry changes to $R\bar{3}$, usually reversing the anisotropy of the expansion along the a and c directions. Alamo [139] has developed a model for the expansion of NZP material in terms of the coupled rotations and distortions of the polyhedra. Composites of NZP, with negative β, and YIG ($Y_3Fe_5O_{12}$), with positive β, have been prepared [140], forming ferrimagnetic zero-expansion ceramics for radar-invisible space mirrors which would not distort with varying exposure to the Sun.

Many other phosphates have negative expansion in at least one direction. For example, corner-sharing NbO_6 octahedra and PO_4 tetrahedra can build up crystals of more than one structure. Tetragonal $NbOPO_4$ [141] has $\alpha_\perp$ and $\alpha_\parallel$ both positive up to a first-order phase transition at about 473 K, above which $\alpha_\perp$ is small and negative. In contrast, monoclinic $NbOPO_4$ has negative expansion in one direction up to a phase transition at 565 K to orthorhombic symmetry, above which the expansion is negative in all directions [142]. Another interesting example is the orthorhombic $Th_4(PO_4)_4P_2O_7$, where it has been suggested that a small negative α_b below room temperature is due to the effect on the network of increasing Coulomb repulsion between two very close (4.19 Å) thorium ions [143].

3.3.12. Metal–organic framework structure. Open framework structures can be formed by metal ions coordinated to polydentate organic ligands. Small negative expansion below room temperature ($\alpha_c \approx -1.5 \times 10^{-6}$ K^{-1}) has been reported [144] for one of these, tetragonal $Sr(C_2(COO)_2)$. The Sr^{2+} ions form a tetrahedral array similar to the diamond structure, and each carbonyl oxygen is linked to two different Sr^{2+} ions.

3.3.13. Polycrystals and composites; microcracking. Polycrystalline and composite materials comprise a vast field beyond our present scope; they are reviewed briefly in chapter 7 of [14]. But we should note that the expansion of such materials can be very different from that of their components. For example, with suitable components and morphology, materials can be formed with negative expansion in at least one direction, although the expansion of each component is wholly positive (e.g. [145]).

Except in polycrystals of a single component, the different expansion coefficients and orientations of neighbouring crystallites give rise to local stresses, which may become severe enough for microcracks to develop. This generally weakens mechanical strength and limits the material's usefulness. It also can alter the bulk expansion drastically, as the cracks open

or close up with changing temperature. This may lead to bulk samples that show negative expansion when net volumetric expansion of the crystallites is actually positive, or enhanced negative expansion [11]. For example, $\beta = -6 \times 10^{-6}\ \mathrm{K}^{-1}$ for single crystals of $Sc_2(WO_4)_3$, but polycrystalline bars have exhibited values as large as $-33 \times 10^{-6}\ \mathrm{K}^{-1}$ [4, 130]. The development of robust new materials with tailorable expansion coefficients and low anisotropy thus presents a considerable challenge to both experimentalist and theorist.

4. Non-vibrational effects

Non-vibrational contributions to thermal expansion usually become dominant only at low temperatures, where vibrational contributions fall off as T^{-3}. But in some materials—especially magnetic—they can be important at higher temperatures also.

4.1. 'Schottky' contributions

Schottky systems within solids are strongly localized. Each system has a finite number of distinct energy levels ε_l. These can arise, for example, by crystal field splitting of electronic or nuclear energy levels, or by tunnelling between alternative atomic sites. The occupation of the energy states is determined by Boltzmann factors $\exp(-\varepsilon_l/kT)$, and thus depends on the intervals between the ε_l (see [14, section 2.5.3]). At very low temperatures all the systems have the lowest energy ε_0. With increasing temperature higher energy states are excited, until all states are equally occupied. The contribution of a single system to the heat capacity thus rises exponentially to a peak—the Schottky 'bump'—and then eventually falls off as T^{-2}. The associated contribution to the thermal expansion depends on how the energy levels depend on volume, as described by Grüneisen factors $\gamma_l = -\mathrm{d}\ln(\varepsilon_l - \varepsilon_0)/\mathrm{d}\ln V$. When energy gaps decrease with pressure, as in the examples below, the contribution to β is negative.

4.1.1. Crystal field splitting. Grüneisen parameters associated with field splitting may be either positive or negative, and are usually of order unity. Figures 15(a) and (b) show the behaviour of two cubic crystals with three-level Schottky systems, caused by the partial splitting of the 4f ground level of the rare earth ion Tm by the crystal electric fields; the levels shown are in units of ε/k with labels Γ_n which denote the symmetry species of the split levels [146]. For TmSb, figure 15(a) shows the magnetic (Schottky) contributions to both the heat capacity and the thermal expansion. They are closely proportional, and indicate that for both excited levels γ_l is about -1.2. For TmTe, figure 15(b) shows the *total* measured expansion coefficient. Here the Grüneisen parameters for the excited levels have different signs: the magnetic contribution is positive at the lowest temperatures, and only becomes negative as the top level is excited, corresponding to $\gamma_{\Gamma_7} = 1.3$, $\gamma_{\Gamma_6} = -1.5$. The expansion becomes positive again above 12 K, owing to vibrational contributions.

At still lower temperatures, similar effects due to the lifting of nuclear degeneracy may occur. Usually only the high temperature end of the Schottky peak is observed in thermal expansion measurements, with a T^{-2} dependence. For the hexagonal metal Pr, Ott [147] found that for $0.5\ \mathrm{K} < T < 2\ \mathrm{K}$

$$\begin{aligned} \alpha_\parallel &= \left[-(9.0 \pm 0.5) \times 10^{-7} T^{-2} + (2 \pm 2) \times 10^{-8} T\right] \mathrm{K}^{-1} \\ \alpha_\perp &= \left[(6.7 \pm 0.5) \times 10^{-7} T^{-2} - (5 \pm 2) \times 10^{-8} T\right] \mathrm{K}^{-1} \end{aligned} \tag{26}$$

corresponding to very large Grüneisen parameters for the nuclear terms: $\gamma_{\parallel,\mathrm{nuc}} = -75$, $\gamma_{\perp,\mathrm{nuc}} = 64$. The terms linear in T are due to the conduction electrons (section 4.3.1). The net volumetric expansion remains negative up to 18 K.

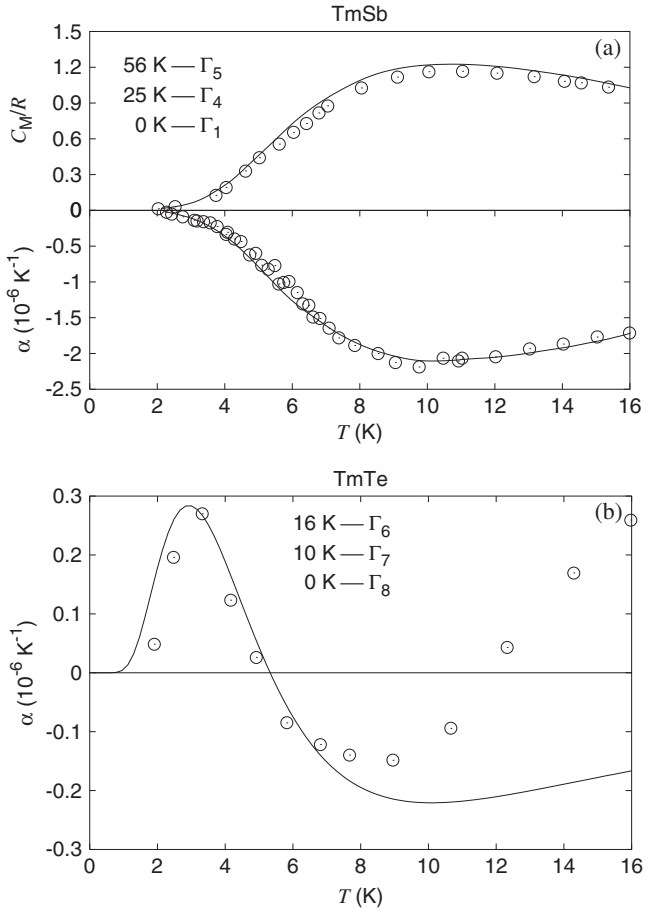

Figure 15. (a) Measured magnetic components of C_P and α for TmSb. Curves are calculated from the levels shown (see the text). The data are taken from [146]. (b) The measured *total* linear expansion coefficient of TmTe at low temperatures. The curve shows the magnetic component as calculated from the levels shown (see the text). The data are taken from [146].

4.1.2. Tunnelling systems. In disordered solids there may be more than one possible site for certain atoms. If the energy barrier between these sites is sufficiently small, quantum tunnelling can occur, thus splitting the atomic ground state energy. The height of the energy barriers is usually very sensitive to changes of volume. Grüneisen parameters are therefore large, and the contribution to the thermal expansion is relatively much greater than that to the heat capacity. For negative expansion, energy barriers between sites need to rise as the volume is *decreased*, so the split levels get closer together and the entropy *increases*.

Tunnelling occurs for some substitutional impurities in alkali halides, and can give rise to either positive or negative thermal expansion. For example, replacement of the anion by 0.03% CN^- in KBr causes the thermal expansion to become *negative* below 0.5 K, with a very large Grüneisen function of about -300 at 0.1 K. Tunnelling occurs between different (111) orientations for the CN^- ion; the negative expansion shows that the orientational barriers increase with pressure [148].

For tunnelling in glasses, see section 2.3.8.

4.2. Molecular rotations

When intermolecular forces are weak, molecules in a solid approximate to free or hindered rotors. Of particular interest are molecules containing symmetrically equivalent H or D atoms, giving rise to different nuclear spin species (such as ortho- and para-hydrogen), each with its system of energy levels. The thermodynamic behaviour of methane and its deuterated compounds provides a rich variety of low temperature anomalies (see [9, p 679]). For example, for CH_4 Heberlein and Adams [149] found α to be negative below 9 K, falling to a minimum of -10×10^{-6} K^{-1} at 7.5 K.

In some systems, as the temperature is lowered the molecules cease to rotate, and instead librate about fixed orientations. The negative expansion of fullerite C_{60} at very low temperatures ($\leqslant$3.4 K) [15] has been interpreted as due to this [150].

4.3. Electronic effects

4.3.1. Conduction electrons. Excitation of electrons at the top of the unfilled conduction band of metals gives rise to a term linear in T in the entropy and heat capacity, which becomes dominant at low temperatures. For the free electron model the corresponding Grüneisen parameter $\gamma^{\mathrm{e}} = 2/3$; and indeed for most real metals the contribution to the thermal expansion is positive. One exception is strontium [151], for which $\gamma^{\mathrm{e}} = -4.4$. It is interesting that a negative γ^{e} has been reported for the quenched disordered alloy Fe_3Al, but not for the ordered crystal [152]. Electronic effects in anisotropic metals are more complex. As we have seen, for Zn the electronic contribution causes $\alpha_\perp$ to become negative again when T falls below 8 K (figure 12), even though both $\gamma^{\mathrm{e}}_\perp$ and $\gamma^{\mathrm{e}}_\parallel$ are positive [71].

For transition metals γ^{e} is again usually positive, although it is negative for the antiferromagnetic metals Cr (-9.3) and Mn (-6.6). But for rare earths and actinides a negative γ^{e} is more common. These metals are mostly non-cubic, and magnetic ordering, nuclear spin and other extra effects make low temperature analysis difficult. α^{e} appears to be negative for polycrystals of La, Ce, Pr, Sm, Nd and Yb [14]. For Pr single crystals, equation (26) gives $\alpha^{\mathrm{e}}_\perp$ as negative, with $\gamma^{\mathrm{e}}_\perp = -4 \pm 2$, $\gamma^{\mathrm{e}}_\parallel = 1.4 \pm 2$. Expansion of the actinide α-U is strongly anisotropic at low temperatures, with an average γ^{e} of -17.9 [153]. Negative α^{e} is sometimes attributed to electron transfer between one band and another (e.g. 4f and 5d for Ce [14]) with consequent volume changes.

At a superconductive transition temperature T_{c} the electronic thermal expansion may change drastically. For example, in the 'normal' state vanadium, niobium and tantalum all have positive expansion. Below T_{c}, for V the positive expansion is enhanced; for Nb the expansion is decreased and at still lower temperatures becomes negative; and for Ta it is negative immediately below T_{c} [154].

4.3.2. Magnetic materials; Invar. Magnetic systems provide some of the most spectacular examples of negative and very low thermal expansion, especially at low temperatures where vibrational contributions are small. Thus for the orthorhombic antiferromagnet $CuCl_2{\cdot}H_2O$ [155] below 10 K the expansion is dominated by a λ transition which peaks at Néel temperature $T_{\mathrm{N}} = 4.4$ K, with α_b negative. Another striking example is the monoclinic perovskite MnF_3 [156], where α_a, α_b and α_c are all negative below $T_{\mathrm{N}} \approx 43$ K. From 20 K up to T_{N}, β is large and negative ($\approx -120 \times 10^{-6}$ K^{-1}), and then is very small up to about 100 K. Since orbital ordering persists to high temperatures, the phenomenon is attributed to spin ordering, as in Invar alloys (see below). Still more complex behaviour is seen in the rare earth metal Ho, with $T_{\mathrm{N}} = 132$ K and two further transitions below 20 K; $\alpha_\parallel$ is negative below T_{N},

undulating between -80 and -25×10^{-6} K^{-1} and then peaking to $\approx -500 \times 10^{-6}$ K^{-1} at the ferromagnetic Curie temperature $T_C = 19.5$ K [157].

The most famous example is the ferromagnetic Invar ($\approx Fe_{65}Ni_{35}$), so-called because of its 'invariable' volume, discovered by Guillaume [158] in 1897 and since then used in the construction of devices where dimensions must be constant over a temperature range near room temperature. β is negative below 30 K (60 K for $Fe_{66}Ni_{34}$ [159]), and then stays below 2×10^{-6} K^{-1} up to nearly 400 K. FePt and FePd alloys behave similarly, and so (to varying extent) do many alloys of Fe–Cr–Ni–Mn–Co. The effect is highly sensitive to composition and generally greatest in alloys with a valence electron/atom ratio of about 8.5 [160, 161].

Why this should be so has remained a subject of controversy [162–164] for over a century. Recent years have seen intensive investigations, exploiting rapid advances in electronic structure theory and its implementation in *ab initio* codes. The effect is due to magnetostriction, i.e. the influence of magnetization on volume. In the wholly ordered ferromagnetic state the electron spins are aligned in parallel. This favours a larger volume, presumably because that reduces the enhanced kinetic energy of the conduction electrons due to band splitting. Thus applying pressure to a state of partial ferromagnetic order causes spins to become less ordered, so contributing positively to $(\partial S/\partial P)_T$ and negatively to the thermal expansion, as in equation (2). This almost cancels the normal vibrational positive contributions, giving very low expansion. The problem is to explain quantitatively (i) why the magnetized state has the larger volume, (ii) why the transition occurs over so wide a temperature range and (iii) why there is a critical dependence on composition. A model for $Fe_{66}Ni_{34}$ [165] with non-collinear spin ordering—i.e. spins tilted at arbitrary angles to the direction of magnetization—accounted qualitatively for the first two of these, and showed also that the magnitude of the local magnetic moment associated with each spin decreased with decreasing magnetic order. Very recent work [166] using a collinear model of spin ordering (spins either 'up' or 'down') has obtained fair quantitative agreement with experiment for FePd, FePt and FeCo systems, including the dependence on composition: magnetic disorder and its effects on the electronic structure determine changes of the local moments, which in turn are primarily responsible for the changes in magnetostriction. The debate continues.

4.3.3. Changes in electron configuration. Particularly striking negative expansion, approximately 40 times larger than that of ZrW_2O_8 over the same temperature range, has been observed for the samarium fulleride $Sm_{2.72}C_{60}$ from 4.2 up to 32 K, when there is an isosymmetric phase transition [167]. Above this temperature the thermal expansivity changes sign and is comparable to that of other metal fulleride salts. The negative expansion is thought to be associated with the availability of two different electronic configurations. These are referred to in a brief review by Sleight [168] as 'mixed electronic configurations', and by Arvanitidis *et al* [167] as 'valence fluctuations'. For Sm they are $4f^6d^0$ and $4f^5d^1$, and the ion is substantially smaller when the d orbital is occupied. Change in the relative amount of each configuration with temperature thus leads to the dramatic decrease in volume with increasing temperature. Similar electronic transitions are thought to be responsible for negative thermal expansion below 60 K in YbCuAl [169] and between 4.2 and 350 K in $Sm_{0.75}Y_{0.25}S$ [170], and for the virtually zero thermal expansion of the metallic compound YbGaGe [171] from 100 to 400 K. In this last example, with increasing temperature electrons are excited from the Yb 4f band to the Ga 4p band, the charge state of the Yb increases from 2+ to 3+ and the size of the Yb decreases. The effect may also occur in pure metals: a fcc phase of Pr has $\alpha \approx -20 \times 10^{-6}$ K^{-1} between 550 and 700 K, attributed to excitation from 4f to 5d [172].

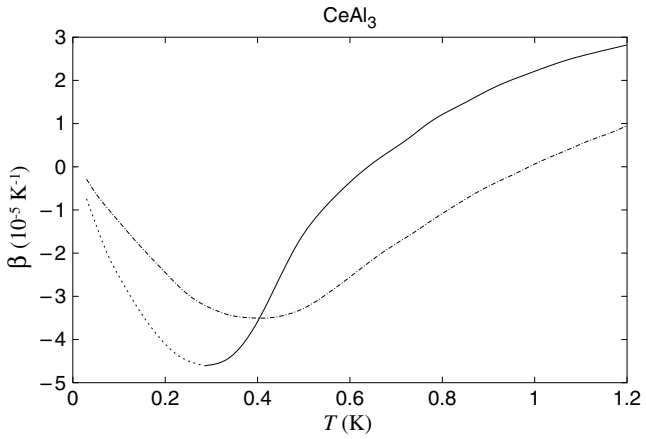

Figure 16. The measured thermal expansion of two different polycrystalline samples of $CeAl_3$. ——, [175]; - - - -, extrapolation towards zero. · — · — ·, [176]. The data are taken from [21].

4.3.4. Highly correlated electron systems. The examples of previous sections illustrate the complicated dependence of the thermal expansion on electronic, magnetic and elastic effects, which are only gradually becoming clearer. Where superconductivity is also involved the mechanisms controlling thermal expansion can be even more complex, particularly in the immediate vicinity of the superconducting transition, and are beyond the scope of this review. This expansion can also be strongly affected by the presence of magnetic fields. We refer the reader to [14] for more details concerning oxide superconductors and to [173] for a discussion of MgB_2.

'Heavy fermion' materials deserve special mention. They present some of the most spectacular effects in thermal expansion seen in any solids, especially at low temperatures [174]. All of them are compounds in which one of the constituent atoms has a partially filled 4f or 5f shell, with high electron correlation. 'Heavy' refers to the effective mass of the conduction electrons, corresponding to large electronic heat capacities that may be two or three orders of magnitude greater than that of Cu. The properties are generally highly strain dependent, and the Grüneisen parameters (positive or negative) can also be very large. The combination of high C_P and high γ leads (see equations (6) and (20)) to electronic thermal expansion that is enormous compared to a typical metal. Behaviour may also be sample dependent. Figure 16 shows the measured expansion of two different polycrystalline samples [175, 176] of the cubic material $CeCl_3$. Below 1 K, β is negative and very large (for Cu at 1 K $\beta = 7 \times 10^{-10}$ K^{-1}); the Grüneisen function varies from about -200 at 0.2 K to 60 at 2 K. The behaviour of most heavy fermion materials is further complicated by anisotropy, and also by magnetic and superconducting transitions; it is highly dependent on the composition. For example, the cubic material UBe_{13} becomes superconducting at 0.9 K. Replacing 3.31% of the uranium by thorium lowers the transition temperature to 0.6 K, below which there now appears a large negative peak in β (-25×10^{-6} K^{-1}) centred at about 0.35 K; this does not destroy the superconductivity [177]. Much remains to be done to unravel the behaviour of these intricate systems [178].

5. Interfaces and nanoparticles

The structure of interfaces and nanoparticles may be very different from that of the bulk material, with consequent changes in the bonding, magnetism and elasticity. In general,

coordination numbers are lower at the surface, where bonds are broken, than in the bulk, and the structure is more open, leading to changes in the thermal expansion. Even in the absence of marked changes in electronic structure, the 'tension effect' (section 2.2.2) might be expected to play a more important role in determining the thermal expansion.

While the study of the static structure of surfaces has reached a point where detailed pictures of multilayer relaxation (and possibly reconstruction) exist, their thermal expansion and the contributions from the different mechanisms that we have discussed are less clear. However, thermal expansion of low index metallic surfaces has recently attracted both experimental and theoretical attention. It is crucial to take into account relaxation and reconstruction and the effect of these on surface phonons. Particular attention has been paid to systems in which the distance between the first two surface atomic layers decreases with increasing temperature. Such behaviour has been observed experimentally [179–181] and studied theoretically [180, 182, 183] for Al(110), Mg($10\bar{1}0$) and Be($10\bar{1}0$). Results for these three surfaces indicate an oscillatory variation perpendicular to the surface, i.e., contractions of the first and third interlayer spacings with increasing temperature accompanied by expansions of the second and fourth interlayer spacings. In contrast, close-packed surfaces such as Mg(0001) are predicted to exhibit increased positive expansion of the spacings between all the outermost layers. For all surfaces, expansion parallel to the surface was positive, as in the bulk. To take account of the additional surface degrees of freedom, an analysis similar to that in section 3 for anisotropic expansion was used. Significant thermal contraction perpendicular to the surface appears to occur only on relatively 'open' faces of metals of low atomic mass.

Thermal expansion of nanoparticles is also under investigation. A particularly interesting study is that of Li *et al* [184], who report a change in sign from positive to negative thermal expansion in cubic Au nanoparticles (4 nm) at $\approx$125 K, with no accompanying change in structure. At the transition, anomalies were also observed in the magnetic response and the heat capacity. This behaviour is thought to be electronic in origin. Thermal contraction independent of electronic effects has been found in classical molecular dynamics simulations of an isolated C_{60} molecule and of a carbon nanotube [185]. Despite the neglect of quantum effects, the expansion varied strongly with temperature (indicating that a quasi-harmonic approximation would be wholly inadequate). The linear expansion coefficient of the C_{60} diameter was negative below about 140 K, becoming as large as -4×10^{-6} K^{-1}. The linear expansion coefficients of both the length and the diameter of the nanotube were negative up to about 800 K, with magnitudes of order 10^{-5} K^{-1}. The simulation was analysed to investigate modes that coupled strongly with the expansion.

6. Final remarks

We have seen that negative thermal expansion has been studied for decades, in a wide range of metallic, inorganic and organic materials. Practical use has been made of the phenomenon in the development of low expansion materials, starting with the discovery of Invar [158] in 1897. The use of Li–Al–Si ceramics in the Corning 'glass ceramic' process has been described [140] as 'one of the most significant breakthroughs in materials processing in 50 years'; millions of casserole dishes, saucepans and stove-tops are made of these ceramics each year. But it was the strongly negative isotropic expansion in ZrW_2O_8 extending up to over 1000 K [1, 2], and its explanation in terms of RUMs [37], that attracted widespread attention and led to a renaissance of interest during the last decade, as witnessed by a stream of publications.

This review has attempted to survey briefly the whole field, particularly emphasizing both basic thermodynamics and mechanisms on the atomic scale that lead to negative expansion. Any contribution to the free energy (vibrational, electronic, nuclear etc) is a function of the

internuclear separations and so affects the thermal expansion. Many of the most interesting examples occur at very low temperatures, and became observable only after the development of highly sensitive techniques of measurement; some low temperature dilatometers are sensitive to length changes of order 1 pm in a macroscopic sample [186]. Such detailed information provides a particularly sensitive test of model interatomic potentials, and more fundamentally of *ab initio* electronic theory. Investigation of vibrational mechanisms has benefited from recent advances in computer power and computational techniques, enabling more complex systems to be studied, using either ad hoc potentials (e.g. [187]) or electronic theory (e.g. [180]) to determine the interatomic forces. Quasi-harmonic lattice dynamics, a technique out of fashion until very recently, has proved particularly useful. It readily takes account of quantum effects that determine low temperature behaviour, mechanisms are easily extracted, and it is often computationally cheap. Molecular dynamics and Monte Carlo simulations are complementary techniques, in that they are applicable at high temperatures where the quasi-harmonic approximation breaks down (e.g. [185]). Investigation of electronic mechanisms has benefited similarly from increased computer power and from development of theory.

There is still much to do. We need a better understanding of many individual materials, including the expansion of surfaces, thin films and microstructures, with the underlying crystal chemistry. In quasi-harmonic theory, efficient methods are needed for computing derivatives of vibrational frequencies with respect to atomic displacements and lattice vectors, which has been carried out using perturbation theory with either potential based models [187] or within density functional theory [180]. Despite recent advances, highly correlated electron systems still lack quantitative and sometimes qualitative understanding. In a totally different area, thermal contraction of proteins, associated with the negative expansion of water, has recently been highlighted [188, 189]. The need for further applied research is evident, especially in the improvement of existing materials and the development of new ones whose expansion matches electronic and biomedical materials while retaining strength and chemical stability. We should note also a new technique of producing negative expansion by cold-rolling of shape-memory alloys [190, 191].

Finally, the mechanisms required to account for negative expansion operate also in other materials. Negative thermal expansion is thus an area ripe for further discoveries of general importance to condensed matter physics.

Acknowledgments

This work was supported by a series of EPSRC grants. GDB acknowledges support from el Consejo Nacional de Investigaciones Científicas y Técnicas de la República Argentina; his contribution to this work was made possible by a visiting Leverhulme Fellowship at Bristol. JAOB's contribution was made possible by Grant X-654 from the University of Buenos Aires and Grant PICT98-D3611 from the Agencia Nacional para la Promoción de la Ciencia y la Tecnología (Argentina).

References

[1] Mary T A, Evans J S O, Vogt T and Sleight A W 1996 *Science* **272** 90
[2] Evans J S O, Mary T A, Vogt T, Subramanian M A and Sleight A W 1996 *Chem. Mater.* **8** 2809
[3] Sleight A W 1998 *Annu. Rev. Mater. Sci.* **28** 29
[4] Evans J S O 1999 *J. Chem. Soc. Dalton Trans.* 3317
[5] Collins J G and White G K 1964 *Prog. Low Temp. Phys.* **4** 450
[6] Barron T H K 1970 *J. Appl. Phys.* **41** 5044
[7] Yates B 1972 *Thermal Expansion* (New York: Plenum)
[8] Krishnan R S, Srinivasan R and Devanarayanan S 1979 *Thermal Expansion of Crystals* (Oxford: Pergamon)

[9] Barron T H K, Collins J G and White G K 1980 *Adv. Phys.* **29** 609
[10] Alamo J and Roy R 1984 *J. Am. Ceram. Soc.* **67** C78
[11] Chu C N, Saka N and Suh N P 1987 *Mater. Sci. Eng.* **95** 303
[12] Roy R, Agrawal D K and McKinstry H A 1989 *Annu. Rev. Mater. Sci.* **19** 59
[13] Agrawal D K 1994 *J. Mater. Ed.* **16** 139
[14] Barron T H K and White G K 1999 *Heat Capacity and Thermal Expansion at Low Temperatures* (New York: Kluwer)
[15] Aleksandrovskii A N, Eselson V B, Manzhelii V G, Udovidchenko B G, Soldatov A V and Sundqvist B 1997 *Low Temp. Phys.* **23** 943
[16] Adenstedt H 1936 *Ann. Phys., Lpz.* **26** 69
[17] Agrawal D K, Roy R and McKinstry H A 1987 *Mater. Res. Bull.* **22** 83
Agrawal D K, Halliyal A and Belsick J 1988 *Mater. Res. Bull.* **23** 159
[18] Ashcroft N W and Mermin N D 1976 *Solid State Physics* (New York: Holt, Rinehart and Winston)
[19] Pippard A B 1964 *The Elements of Classical Thermodynamics* (Cambridge: Cambridge University Press)
[20] Grüneisen E 1926 *Handb. Phys.* **10** 1
[21] Barron T H K 1998 *Thermal Expansion of Solids* (*CINDAS Data Series on Material Properties* vol I-4, ed C Y Ho) ed R E Taylor (Materials Park, OH: ASM International) chapter 1
[22] Born M and Huang K 1954 *Dynamical Theory of Crystal Lattices* (Oxford: Clarendon)
[23] Barron T H K and Klein M L 1974 *Dynamical Properties of Solids* vol 1, ed G K Horton and A A Maradudin (Amsterdam: North-Holland) chapter 7
[24] Fornasini P 2001 *J. Phys.: Condens. Matter* **13** 7859
[25] Barron T H K and Gibbons T G 1974 *J. Phys. C: Solid State Phys.* **7** 3260
Barron T H K and Gibbons T G 1974 *J. Phys. C: Solid State Phys.* **7** 3269
Barron T H K and Gibbons T G 1974 *J. Phys. C: Solid State Phys.* **7** 3287
[26] Barron T H K 1955 *Phil. Mag.* **46** 720
[27] Barron T H K 1957 *Ann. Phys.* **1** 77
[28] Bruno J A O, Allan N L, Barron T H K and Turner A D 1998 *Phys. Rev.* B **58** 8416
[29] Blackman M 1958 *Phil. Mag.* **3** 831
[30] Sikka S K 2004 *J. Phys.: Condens. Matter* **16** S1033
[31] Simon M E and Varma C M 2001 *Phys. Rev. Lett.* **86** 1781
[32] Phillips J C 1970 *Rev. Mod. Phys.* **42** 317
[33] White M A, Lushington K J and Morrison J A 1978 *J. Chem. Phys.* **69** 4227
[34] Schafer W and Kirfel A 2002 *Appl. Phys.* A **74** S1010
[35] Tiano W, Dapiaggi M and Artioli G 2003 *J. Appl. Crystallogr.* **36** 1461
[36] a Beccara S, Dalba G, Fornasini P, Grisenti R and Sanson A 2002 *Phys. Rev. Lett.* **89** 025503
[37] Pryde A K A, Hammonds K D, Dove M T, Heine V, Gale J D and Warren M C 1996 *J. Phys.: Condens. Matter* **8** 10973
[38] Giddy A P, Dove M T, Pawley G S and Heine V 1993 *Acta Crystallogr.* A **49** 697
[39] Pryde A K A, Dove M T and Heine V 1998 *J. Phys.: Condens. Matter* **10** 8417
[40] Welche P L R, Heine V and Dove M T 1998 *Phys. Chem. Miner.* **26** 63
[41] Heine V, Welche P R L and Dove M T 1999 *J. Am. Ceram. Soc.* **82** 1793
[42] Dove M T, Hammonds K D, Harris M J, Heine V, Keen D A, Pryde A K A, Trachenko K and Warren M C 2000 *Miner. Mag.* **64** 377
[43] Tao J Z and Sleight A W 2003 *J. Phys. Chem. Solids* **64** 1473
[44] Ernst G, Broholm C, Kowach G R and Ramirez A P 1998 *Nature* **396** 147
[45] Mittal R, Chaplot S L, Schober H and Mary T A 2001 *Phys. Rev. Lett.* **86** 4692
[46] Ramirez A P and Kowach G R 1998 *Phys. Rev. Lett.* **80** 4903
[47] Mittal R and Chaplot S L 1999 *Phys. Rev.* B **60** 7234
[48] Ravindran T R, Arora A K and Mary T A 2000 *Phys. Rev. Lett.* **84** 3879
[49] Cao D, Bridges F, Kowach G R and Ramirez A P 2002 *Phys. Rev. Lett.* **89** 215902
[50] Drymiotis F R, Ledbetter H, Betts J B, Kimura T, Lashley J C, Migliori J C, Ramirez A, Kowach G and Van Duijn J 2004 *Phys. Rev. Lett.* **93** 025502
[51] David W I F, Evans J S O and Sleight A W 1999 *Europhys. Lett.* **46** 661
[52] Allen S and Evans J S O 2003 *Phys. Rev.* B **68** 134101
[53] Nakajima N, Yamamura Y and Tsuji T 2003 *Solid Sate Commun.* **128** 193
[54] Korthuis V, Khosrovani N, Sleight A W, Roberts N, Dupree R and Warren W W 1995 *Chem. Mater.* **7** 412
[55] Taylor D 1984 *Br. Ceram. Trans. J.* **83** 129
[56] Khosrovani N, Korthuis V, Sleight A W and Vogt T 1996 *Inorg. Chem.* **35** 485

[57] Carlson S and Krogh Andersen A M 2001 *J. Appl. Crystallogr.* **34** 7
[58] Yamahara K, Okazaki K and Kawamura K 2001 *J. Non-Cryst. Solids* **291** 32
[59] Achary S N, Jayakumar O D, Tyagi A K and Kulshresththa S K 2003 *J. Solid State Chem.* **176** 37
[60] Couves J W, Jones R H, Parker S C, Tschaufeser P and Catlow C R A 1993 *J. Phys.: Condens. Matter* **5** L329
[61] Tschaufeser P and Parker S C 1995 *J. Phys. Chem.* **99** 10609
[62] Attfield M P and Sleight A W 1998 *Chem. Commun.* 601
[63] Huang L P and Kieffer J 2004 *Phys. Rev.* B **69** 224204
[64] Phillips W A 1972 *Low Temp. Phys.* **7** 351
[65] Anderson P W, Halperin B I and Varma C M 1972 *Phil. Mag.* **25** 1
[66] Molina M I and Mattis D C 1991 *Phys. Lett.* A **159** 337
[67] Bailey A C and Yates B 1970 *J. Appl. Phys.* **41** 5088
[68] Barron T H K and Gibbons T G 1974 *J. Phys. C: Solid State Phys.* **7** 3287
[69] Barron R M, Barron T H K, Mummery P M and Sharkey M 1988 *Can. J. Chem.* **66** 718
[70] Thurston R N 1964 *Physical Acoustics* vol 1A, ed W P Mason (New York: Academic) p 1
[71] Barron T H K and Munn R W 1967 *Phil. Mag.* **15** 85
[72] Barron T H K and Munn R W 1970 *Pure Appl. Chem.* **22** 527
[73] Wallace D C 1970 *Solid State Phys.* **25** 301
[74] Munn R W 1972 *J. Phys. C: Solid State Phys.* **5** 535
[75] Wallace D C 1972 *Thermodynamics of Crystals* (New York: Wiley)
[76] Hearmon R F S 1979 *Landolt–Börnstein* vol III/11, ed K-H Hellwege (Berlin: Springer) chapter 1
[77] Ibach H 1969 *Phys. Status Solidi* **33** 257
[78] Yates B, Cooper R F and Kreitman M M 1971 *Phys. Rev.* B **4** 1314
[79] Dantl G 1962 *Z. Phys.* **166** 115
[80] Riley D P 1945 *Proc. Phys. Soc.* **57** 486
[81] Kellet E A and Richards B P 1964 *J. Nucl. Mater.* **12** 184
[82] Yates B, Overy M J and Pirgon O 1975 *Phil. Mag.* **32** 847
[83] White G K 1972 *J. Phys. C: Solid State Phys.* **5** 2731
[84] Taylor J B, Bennett S L and Heyding R D 1965 *J. Phys. Chem. Solids* **26** 69
[85] Munn R W 1969 *Adv. Phys.* **18** 515
[86] Soriano M R, Barrera G D and Allan N L 2001 *Chem. Phys. Lett.* **350** 543
[87] Baughman R H 1973 *J. Chem. Phys.* **58** 2976
Gibbons T G 1974 *J. Chem. Phys.* **60** 1094
[88] Grosse R, Krause P, Meissner M and Tausend A 1978 *J. Phys. C: Solid State Phys.* **11** 45
[89] Arnold U and Grosse P 1968 *Phys. Status Solidi* **28** K93
[90] Gibbons T G 1973 *Phys. Rev.* B **7** 1410
[91] Lacks D J and Rutledge G C 1994 *J. Phys. Chem.* **98** 1222
[92] Lacks D J and Rutledge G C 1994 *Macromolecules* **27** 7197
[93] Lacks D J and Rutledge G C 1995 *Macromolecules* **28** 1115
[94] Tasumi M and Simanouchi T 1965 *J. Chem. Phys.* **43** 1245
[95] Dadobaev G and Slutsker A I 1981 *Sov. Phys.—Solid State* **23** 1131
[96] White G K and Choy C L 1984 *J. Polym. Sci. Polym. Phys. Edn* **22** 835
[97] White G K, Smith T F and Birch J A 1976 *J. Chem. Phys.* **65** 554
[98] White G K, Collocott S J and Collins J G 1990 *J. Phys.: Condens. Matter* **2** 7715
[99] Li J, Yokochi A, Amos T G and Sleight A W 2002 *Chem. Mater.* **14** 2602
[100] Krivovichev S V, Filatov S K and Burns P C 2002 *Can. Mineral.* **40** 1185
[101] White G K and Roberts R B 1988 *Aust. J. Phys.* **41** 791
[102] Stevens R, Woodfield B F, Boerio-Goates J and Crawford M K 2004 *J. Chem. Thermodyn.* **36** 349
[103] Wright A F 1976 *4th Int. Conf. on Phys. Non-Crystalline Solids* ed G H Frischat (Aedermannsdorf, Switzerland: Trans. Tech. Publications) p 598
[104] Wright A F and Lehmann M S 1981 *J. Solid State Chem.* **36** 371
[105] Kihara K 2001 *Phys. Chem. Miner.* **28** 365
[106] Smirnov M B 1999 *Phys. Rev.* B **59** 4036
[107] Barron T H K and Pasternak A 1987 *J. Phys. C: Solid State Phys.* **20** 215
[108] Aliouane N, Gagou Y, Elkaim E, Lauriat J P, Badeche T and Saint-Gregoire P 2002 *Ferroelectrics* **269** 279
[109] Kosten K and Arnold H 1980 *Z. Kristallogr.* **152** 119
[110] Mittal R, Chaplot S L, Kolesnikov A I, Loong C-K, Jayakumar O D and Kulshreshtha S K 2002 *Phys. Rev.* B **66** 174304
[111] Chang Z-P and Barsch G R 1976 *IEEE Trans. Sonics Ultrason.* **23** 127

[112] Gale J D 1998 *J. Phys. Chem.* B **102** 5423
[113] Lightfoot P, Woodcock D A, Maple M J, Villaescusa L A and Wright P A 2001 *J. Mater. Chem.* **11** 212
[114] Tao J Z and Sleight A W 2003 *J. Phys. Chem. Solids* **64** 1473
[115] Villaescusa L A, Lightfoot P, Teat S J and Morris R E 2001 *J. Am. Chem. Soc.* **123** 5453
[116] Bull I, Lightfoot P, Villaescusa L A, Bull L M, Gover R K B, Evans J S O and Morris R E 2003 *J. Am. Chem. Soc.* **125** 4342
[117] Marinkovic B A, Jardim P M, Saavedra A, Lau L Y, Baehtz C, de Avillez R R and Rizzo F 2004 *Microporous Mesoporous Mater.* **71** 117
[118] Evans J S O, Hu Z, Jorgensen J D, Argyriou D N, Short S and Sleight A W 1997 *Science* **275** 61
[119] Jorgensen J D, Hu Z, Teslic S, Argyriou D N, Short S, Evans J S O and Sleight A W 1999 *Phys. Rev.* B **59** 215
[120] Abrahams S C 1966 *J. Chem. Phys.* **45** 2745
[121] Evans J S O, Mary T A and Sleight A W 1998 *J. Solid State Chem.* **137** 148
[122] Evans J S O and Mary T A 2000 *Int. J. Inorg. Mater.* **2** 143
[123] Evans J S O, Mary T A and Sleight A W 1998 *Physica* B **241–243** 311
[124] Tyagi A K, Achary S N and Mathews M D 2002 *J. Alloys Compounds* **339** 207
[125] Forster P M, Yokochi A and Sleight A W 1998 *J. Solid State Chem.* **140** 157
[126] Woodcock D A, Lightfoot P and Ritter C 2000 *J. Solid State Chem.* **149** 92
[127] Sumithra S and Umarji A M 2003 *Proc. Indian Acad. Sci. Chem. Sci.* **115** 695
[128] Evans J S O, Mary T A and Sleight A W 1997 *J. Solid State Chem.* **133** 580
[129] Imanaka N, Hiraiwa M, Adachi G, Dabkowska H and Dabkowski A 2000 *J. Cryst. Growth* **220** 176
[130] Mary T A and Sleight A W 1999 *J. Mater. Res.* **14** 912
[131] Shen R and Wang T M 2004 *Rare Metal Mater. Eng.* **33** 91
[132] Hummel F A 1948 *Foote Prints Chemicals Metals Alloys Ores* **20** 3
[133] Hummel F A 1951 *J. Am. Ceram. Soc.* **34** 235
[134] Collocot S J 1985 *J. Non-Cryst. Solids* **70** 291
[135] Woodcock D A, Lightfoot P and Smith R I 1998 *Mater. Res. Soc. Symp. Proc.* **547** 191
[136] Limaye S Y, Agrawal D K and McKinstry H A 1987 *J. Am. Ceram. Soc.* **70** C232
[137] Roy R, Agrawal D K, Alamo J and Roy R A 1984 *Mater. Res. Bull.* **19** 471
[138] Woodcock D A, Lightfoot P and Ritter C 1998 *Chem. Commun.* 107
[139] Alamo J 1993 *Solid State Ion.* **63–65** 547
[140] Roy R and Agrawal D K 1997 *Nature* **388** 433
[141] Amos T G, Yokochi A and Sleight A W 1998 *J. Solid State Chem.* **141** 303
[142] Amos T G and Sleight A W 2001 *J. Solid State Chem.* **160** 230
[143] Launay S, Wallez G and Quarton M 2001 *Chem. Mater.* **13** 2833
[144] Hohn F, Pantenburg I and Ruschewitz U 2002 *Chem. Eur. J.* **8** 4536
[145] Landert M, Kelly A, Stearn R J and Hine P J 2004 *J. Mater. Sci.* **39** 3563
[146] Ott H R and Lüthi B 1977 *Z. Phys.* B **28** 141
[147] Ott H R 1975 *Solid State Commun.* **16** 1355
[148] Dobbs J N, Foote M C and Anderson A C 1986 *Phys. Rev.* B **33** 4178
[149] Heberlein D C and Adams E D 1970 *J. Low Temp. Phys.* **3** 115
[150] Loktev V M 1999 *Low Temp. Phys.* **25** 823
[151] White G K 1972 *J. Phys. F: Met. Phys.* **2** 865
[152] Mukherjee G D, Bansal C and Chatterjee A 1996 *Phys. Rev. Lett.* **76** 1876
[153] Andres K 1968 *Phys. Rev.* **170** 614
[154] White G K 1962 *Cryogenics* **2** 292
[155] Harding G L, Lanchester P C and Street R 1971 *J. Phys. C: Solid State Phys.* **4** 2923
[156] Hunter B A, Kennedy B J and Vogt T 2004 *Phys. Rev.* B **69** 020410
[157] White G K 1989 *J. Phys.: Condens. Matter* **1** 6987
[158] Guillaume C E 1897 *C. R. Acad. Sci.* **125** 235
[159] Collocott S J and White G K 1986 *Cryogenics* **26** 402
[160] Wasserman E F 1989 *Phys. Scr.* T **25** 209
[161] Wasserman E F 1990 *Ferromagnetic Materials* vol 5, ed K H J Buschow and E P Wohlfarth (Amsterdam: North-Holland) chapter 3
[162] Wassermann E F 1991 *J. Magn. Magn. Mater.* **100** 346
[163] Shiga M 1994 *Material Science and Technology* Part II, vol 3B, ed R W Cahn, P Haasen and E J Kramer (Weinheim: VCH) p 159
[164] Wassermann E F 1997 *The Invar Effect: a Centennial Symposium* ed J Wittenauer (Warrendale, PA: Minerals, Metals and Materials Society) p 51

[165] van Schilfgaarde M, Abrikosov I A and Johansson B 1999 *Nature* **400** 46
[166] Khmelevskyi S, Turek I and Mohn P 2003 *Phys. Rev. Lett.* **91** 037201
Khmelevskyi S and Mohn P 2004 *Phys. Rev.* B **69** 140404
[167] Arvanitidis J, Papagelis K, Margadonna S, Prassides K and Fitch A N 2003 *Nature* **425** 599
[168] Sleight A 2003 *Nature* **425** 674
[169] Mattens W C M, Hölscher H, Tuin G J M, Moleman A C and de Boer F R 1980 *J. Magn. Magn. Mater.* **15–18** 982
[170] Mook H and Holtzberg F 1981 *Valence Fluctuations in Solids* ed L M Falicov, W Hanke and M B Maple (Amsterdam: North-Holland) p 113
[171] Salvador J R, Guo F, Hogan T and Kanatzidis M G 2003 *Nature* **425** 702
[172] Kuznetsov A Yu, Dmitriev V P, Bandilet O I and Weber H-P 2003 *Phys. Rev.* B **68** 064109
[173] Anshukova N V, Bulychev B M, Golovashkin A I, Ivanova L I, Krynetskii I B, Minakov A A and Rusakov A P 2003 *J. Exp. Theor. Phys.* **97** 70
[174] Ott H R 1987 *Prog. Low Temp. Phys.* **11** 215
[175] Andres K, Graebner J E and Ott H R 1975 *Phys. Rev. Lett.* **35** 1779
[176] Ribault M, Benoit A, Flouquet J and Palleau P 1979 *J. Physique Lett.* **40** L413
[177] Ott H R, Rudigier H, Fedder E, Fisk Z and Smith J L 1986 *Phys. Rev.* B **33** 126
[178] Springford M 1997 *Electron, a Centenary Volume* ed M Springford (Cambridge: Cambridge University Press) chapter 8
[179] Mikkelsen A, Jiruse J and Adams D L 1999 *Phys. Rev.* B **60** 7796
Busch B W and Gustafsson T 2000 *Phys. Rev.* B **61** 16097
[180] Ismail, Plummer E W, Lazzeri M and de Gironcoli S 2001 *Phys. Rev.* B **63** 233401
[181] Ismail, Hofmann Ph, Baddorf A P and Plummer E W 2002 *Phys. Rev.* B **66** 245414
[182] Marzari N, Vanderbilt D, De Vita A and Payne M C 1999 *Phys. Rev. Lett.* **82** 3296
[183] Lazzeri M and de Gironcoli S 2002 *Phys. Rev.* B **65** 245402
[184] Li W-H, Wu S Y, Yang C C, Lai S K, Lee K C, Huang H L and Yang H D 2002 *Phys. Rev. Lett.* **89** 135504
[185] Kwon Y-K, Berber S and Tománek D 2004 *Phys. Rev. Lett.* **92** 015901
[186] Swenson C A 1998 *Thermal Expansion of Solids* (*CINDAS Data Series on Material Properties* vol I-4, ed C Y Ho) ed R E Taylor (Materials Park, OH: ASM International) chapter 8
[187] Taylor M B, Barrera G D, Allan N L and Barron T H K 1997 *Phys. Rev.* B **56** 14380
Taylor M B, Barrera G D, Allan N L, Barron T H K and Mackrodt W C 1998 *Comput. Phys. Commun.* **109** 135
[188] Melchiona S, Briganti G, Londei P and Cammarano P 2004 *Phys. Rev. Lett.* **92** 158101
[189] Pan Y S, Birkedal H, Pattison P, Brown D and Chapuis G 2004 *J. Phys. Chem.* B **108** 6458
[190] Kainuma R, Wang J J, Omori T, Sutou Y and Ishida K 2002 *Appl. Phys. Lett.* **80** 4348
[191] Zel'dovich V I, Frolova N Y, Khomskaya I V and Epanechnikov E A 2003 *J. Physique* IV **112** 773